AD-772 513

ASPECTS OF MECHANICAL BEHAVIOR OF ROCK UNDER STATIC AND CYCLIC LOADING. PART B: MECHANICAL BEHAVIOR OF ROCK UNDER CYCLIC LOADING

Bezalel C. Haimson

Wisconsin University

Prepared for:

Advanced Research Projects Agency
Bureau of Mines

April 1973

AD772 513

3200.8 (Att 1 to Encl 1)
Mar 7, 66

DOCUMENT CONTROL DATA - R & D

(Security classification of title, body of abstract and indexing annotation must be entered when the overall report is classified)

1. ORIGINATING ACTIVITY (Corporate author)

Dept. of Metallurgical and Mineral Engineering
University of Wisconsin
Madison, WI 53706

2a. REPORT SECURITY CLASSIFICATION

Unclassified

2b. GROUP

3. REPORT TITLE

"Mechanical Behavior of Rock Under Cyclic Loading", Part B of "Aspects of Mechanical Behavior of Rock Under Static and Cyclic Loading"

4. DESCRIPTIVE NOTES (Type of report and inclusive dates)

Final Report (March 1, 1972 - February 28, 1973)

5. AUTHOR(S) (First name, middle initial, last name)

Bezalel C. Haimson

6. REPORT DATE	7a. TOTAL NO. OF PAGES	7b. NO. OF REFS
March 1973	84	6

8a. CONTRACT OR GRANT NO.

H0220041

b. PROJECT NO.

c. 1579, Amendment 3

d.

9a. ORIGINATOR'S REPORT NUMBER(S)

9b. OTHER REPORT NO(S) (Any other numbers that may be assigned this report)

10. DISTRIBUTION STATEMENT

Distribution of this document is unlimited

11. SUPPLEMENTARY NOTES

12. SPONSORING MILITARY ACTIVITY

ARPA

13. ABSTRACT

The study of the mechanical behavior of hard rock types under cyclic uniaxial compression and tension was continued and a program of cyclic triaxial compression and uniaxial tension-compression was initiated. All rocks (granite, sandstone, limestone, marble) exhibited cyclic fatigue characteristics in both tension and compression with fatigue strengths of 55-70% within 10^5-10^6 cycles. In cyclic tension-compression the fatigue strength reduced to 30% at 10^5 cycles. Prefailed granite exhibited substantial fatigue endurance. An inter-relationship between compression fatigue and the complete stress-strain curve has been demonstrated. For the same maximum stress cyclic stress amplitudes appear to affect fatigue life. In particular, indications are the compression-tension cyclic loading could be most damaging. The process of fabric deterioration due to fatigue is localized in cyclic tension unlike cyclic compression where it affects the entire body subjected to repetitive loading. As a practical application of the S-N curves obtained, it is recommended that the appropriate fatigue strength at 10^5 cycles be used as the effective rock strength in design of structures in intact rock. The permanent strain after one cycle in tension and the complete stress-strain in compression could be used to estimate maximum allowable permanent deformation prior to cyclic fatigue. The fatigue strength of failed rock should not be overlooked in designing underground structures.

DD FORM 1473

Security Classification

Security Classification

14. KEY WORDS	LINK A		LINK B		LINK C	
	ROLE	WT	ROLE	WT	ROLE	WT
Rock Mechanics						
Fatigue in Rock						
Cyclic Loading in Rock						
S-N Curves						
Complete Stress-Strain Curves						
Cyclic Tension						
Cyclic Compression						
Cyclic Tension-Compression						
Rock Strength						
Rock Young's Modulus						
Design in Rock						
Microfracture in Rock						
Failure Mechanism						

Security Classification

ASPECTS OF MECHANICAL BEHAVIOR OF ROCK UNDER STATIC AND CYCLIC LOADING

PART B: MECHANICAL BEHAVIOR OF ROCK UNDER CYCLIC LOADING

FINAL REPORT
April 1973

by

B. C. Haimson
Co-Principal Investigator
(608)-262-2563

Department of Metallurgical and Mineral Engineering
and the
Engineering Experiment Station
College of Engineering
The University of Wisconsin
Madison, Wisconsin 53706

Sponsored by Advanced Research Project Agency

ARPA Order No. 1579, Amendment 3
Program Code No. 2F10
Contract No. H0220041
Contract Period: March 1972 through April 1973
Total Amount of Contract: $50,000

PREFACE

This final report covers the accomplishments of the second year period in the research program entitled "Mechanical Behavior of Rock Under Cyclic Loading", B. C. Haimson, Principal Co-Investigator. The program is Part B of a project entitled, "Aspects of Mechanical Behavior of Rock Under Static and Cyclic Loading" (Contract H0220041). The report on Part A of the project is published in a separate volume. For completion purposes the present report should be viewed as a continuation of the annual report submitted in June 1972 under contract H022004.

ACKNOWLEDGMENTS

The reported research was monitored by the Twin Cities Mining Research Center, U. S. Bureau of Mines. Dr. Syd Peng was the Technical Project Officer.

The graduate research assistants who performed most of the reported experimental work were V. Rajaram, T. Tharp and K. Kim.

TABLE OF CONTENTS

LIST OF FIGURES AND TABLES

SUMMARY

The reported investigation is the continuation of an extensive study of the cyclic fatigue phenomenon in hard rock. This is the phenomenon of premature failure occurring in materials subjected to cyclic or repetitive loading. A thorough understanding of rock mechanical reaction to such loading could help in the design of safe rock structures and has the potential of improving rock breaking methods.

The main objectives of the project during the reported period were to study the mechanical behavior of additional hard rock types under cyclic uniaxial compression and tension, and initiate a program of cyclic triaxial compression and uniaxial tension-compression testing.

S-N curves were obtained for Berea sandstone and Westerly granite in uniaxial compression, for Indiana limestone, Westerly granite and Berea sandstone in uniaxial tension, for Westerly granite in triaxial compression (confining pressures of 1,000 psi and 2,500 psi), and for Westerly granite in tension-compression (stress range of 10,000 psi). All rocks exhibited cyclic fatigue characteristics in both tension and compression with fatigue strengths of 55-70% within 10^5-10^6 cycles. In tension-compression the fatigue strength at 10^5 cycles was as low as 30% of the tensile strength. All these results reinforce the assertion that hard rock is fatigue prone. Design of structures in rock should not ignore the effects of repetitive loading. The fatigue strengths of each rock as determined by the reported tests could be used as the effective strengths of intact rock. Since not every rock in the field can be extensively tested, it is recommended that a value of 50% of the appropriate static strength (compressive or tensile) be used as the effective strength in the design of structures to be subjected to compression or tension only. If tension-compression type loading is expected the effective strength will have to be further reduced. Preliminary tests indicate a value of 25% of the appropriate static strength could be adequate. The discovery of the extremely reduced fatigue strength in tension-compression could and should be used to advantage in rock breaking.

Cyclically compressed sandstone and granite specimens that had been previously "failed", exhibited substantial fatigue endurance, although the fatigue life at each stress level was reduced when compared with unprefailed rock. These results could be extremely useful to the design of structures where rock might have previously been deformed to beyond the limit corresponding to its compressive strength. Pillars, ribs or other structural components although failed could resist cyclic loading to an extent determined by appropriate S-N curves.

Additional experimental evidence was collected in support of an interrelationship between rock compression fatigue and the respective complete stress-strain curve. Particularly in granite, the amount of permanent deformation exhibited by the upper peak strain in stress-controlled tests, the shape of the S-N curve, the amount of peak stress relaxation and the type of fatigue failure in strain controlled tests, all allude to a Class II rock type and match the characteristics of the complete stress-strain curve. The practical application of these results could be substantial. Determining the complete stress-strain curve for a rock is much easier and less time consuming than preparing an S-N curve. Monitoring the amount of accumulated permanent deformation at a particular stress level (whether in a laboratory specimen or an underground structure) and comparing it with the allowable magnitude from the complete stress-strain curve could establish the stability condition and estimate the amount of cyclic loading that the rock can still withstand. The shape of the complete stress-strain curve could indicate the ranges of maximum stress for which the rock is more susceptible to fatigue effects. These are the regions of minimum allowable permanent strain, usually caused by those portions of the descending stress-strain curve having positive slopes.

In uniaxial tension the S-N curves of all four rock types tested are represented by straight lines closely approximated by $S = 100\% - 7 \log N$ (in terms of percentage of respective tensile strength). This result implies that the equation could represent most other hard rock types, in which case no further testing of these rocks is required. Stress-strain curves in uniaxial tension reveal that the permanent strain after one cycle is relatively very large and approximately one half of the total

permanent strain prior to fatigue failure. This finding could be used advantageously to predict total permanent deformation related to fatigue in tension without actually cyclically testing a rock.

In cyclic tension-compression the tangential Young's modulus decreased by some 30% between the first and the last loading cycles. This "softening" phenomenon was not encountered in other modes of cyclic loading, and could be related to the same mechanism that makes tension-compression the most damaging cyclic loading.

The previously reported investigation of the compression fatigue mechanism showed that the process of cumulative damage was spread through the entire specimen. In uniaxial tension fatigue, however, fabric changes due to cyclic loading appear to be very localized, i.e., a few of the more crucial existing microcracks slowly enlarge until one gains on the others, propagates and splits the specimen. Other than the very close vicinity of the rupture plane no changes were observed in the internal structure of the rock. The implication here is that, unlike compression fatigue, impending tensile fatigue failure may give little warning in terms of deformation away from the critical flaw.

In conclusion, it is felt that the basic mechanical response of hard rock to cyclic loading has been established. Additional work to consolidate some of the results and to investigate more closely practical applications in both design and rock breaking is strongly recommended.

INTRODUCTION

Rock formations as well as rock structures are subjected to both static and dynamic loads. Static loads result from such sources as tectonic forces and the weight of the overlying rock. Small dynamic loads are continually propagated through natural vibrations of the earth's crust. Large dynamic loads are intermittently applied through major earthquakes, rock blasting, drilling, traffic, etc. The mechanical behavior of rock under static loading has been thoroughly investigated. However, rock reaction to the cyclic, pulsating stresses resulting from dynamic loads has been generally neglected with the exception of a few rather limited studies. It is a known fact that cyclic loading often causes a material to fail prematurely at a stress level lower than its determined strength under monotonic conditions. This phenomenon is commonly termed "fatigue". Tunnel walls, excavation roofs and ribs, bridge abutments, dam and road foundations are only a few of the rock structures that can be weakened by repetitive loading. Better understanding of cyclic fatigue may assist the engineer in preparing a more rational design that will eliminate premature failures. On the other hand, knowledge of fatigue characteristics may help improve rock breaking methods, e.g., drilling and blasting. It is, therefore, imperative that the effect of pulsating stresses on rock is fundamentally studied with the ultimate goal of deriving practical applications.

Such a study is now underway at the University of Wisconsin, and the present report covers the second year period of a program to investigate the mechanical behavior of rock under cyclic loading. In the first year a thorough literature survey was carried out and an extensive experimental investigation was initiated (1). White Tennessee marble, Georgia marble and Indiana limestone were tested under cyclic uniaxial compression, Pink and White Tennessee marble were tested under cyclic tension.

The main results of the first year program were:

1. All tested rocks were weakened by cyclic loading whether under compression or tension, if the lower peak load was near zero, and the upper peak load was held at a level

above a threshold, typical to the particular rock. The threshold appeared to be within the inelastic range of the stress-strain characteristics.

2. "Failed" marble exhibited substantial strength under cyclic compression.
3. In cyclic uniaxial compression both the axial and lateral strains underwent large permanent strains (cyclic creep). The average Young's modulus decreased some during the test; the Poisson's ratio increased. The volumetric strain underwent cyclic compression dilatancy.
4. The amount of cyclic creep between the first and the last cycle appeared to be limited by the complete stress-strain curve.
5. Fabric analysis was conducted in cyclic compression specimens using stress-strain data, acoustic emission, optical diffraction techniques, and a photomicrographic study. The indication was that microcracking initiated during the very first cycle, and some cycles thereafter. A steady state period followed, characterized by a near stagnation in crack initiation. Thereafter, a period of crack extension and coalescence, culminated in crack propagation and faulting. Within the above frame of fatigue mechanism, differences were observed between the non-porous marble and the high porosity (14%) limestone (1).

Based on the above results a number of practical applications were suggested. The qualification was made, however, that more experimental work was needed to (a) confirm the obtained results in other rock types, (b) to investigate other loading configurations and (c) simulate more realistic rock conditions.

The present report covers the work performed in the second year period of the project. Results are presented of cyclic fatigue studies of two additional rocks in uniaxial compression, three additional rocks in cyclic tension, and one rock in both triaxial compression and tension-compression. Further studies into the mechanism of fatigue and its relationship to other material properties are also presented and discussed.

LABORATORY EQUIPMENT AND EXPERIMENTAL PROCEDURES

Rock Description

The rocks tested during the reported stage of the program were Indiana limestone, Pink Tennessee marble, Berea sandstone and Westerly granite. The first two rocks were described in the annual report (1). A brief description of the other two follows:

Berea sandstone is light gray in color, and consists of 99% quartz. It is finely grained, very porous (∿19%), and has visible bedding planes.

Westerly granite has very low porosity (∿1%) and fine grain size. It contains approximately equal amounts of quartz, microcline and plagioclase, and 5% biotite.

Specimen Preparation

All the specimens used in the present phase of the program were 1.0 in. in diameter, 2.5 in. long and were prepared as detailed in the first annual report (1).

Apparatus

The two servo-controlled loading machines and the additional apparatus used in uniaxial cyclic compression and tension testing were previously described (1). To facilitate strain measurements in cyclic tension, a double HP24 DCDT device was used as shown in Fig. 1. For cyclic tension-compression the set-up used was identical to that utilized for uniaxial cyclic tension, except that the endcaps were hardened so they could take high compressive stresses.

The triaxial compression cyclic tests were run in a specially constructed triaxial cell using the MTS machine (Fig. 2). The triaxial cell is a modified design of a cell first described by Paterson (2). It has a bore of 2.0 in. and the capability of applying up to 15,000 psi confining pressures to 1.0 in. x 2.5 in. cylindrical specimens. Two 1.0 in. diameter pistons at either end of the cell are rigidly connected by a yoke. The lower piston transmits the load from the hydraulic ram to the specimen. The upper piston is forced by the yoke to move with the lower piston, thus allowing the confining oil to maintain its volume approximately constant.

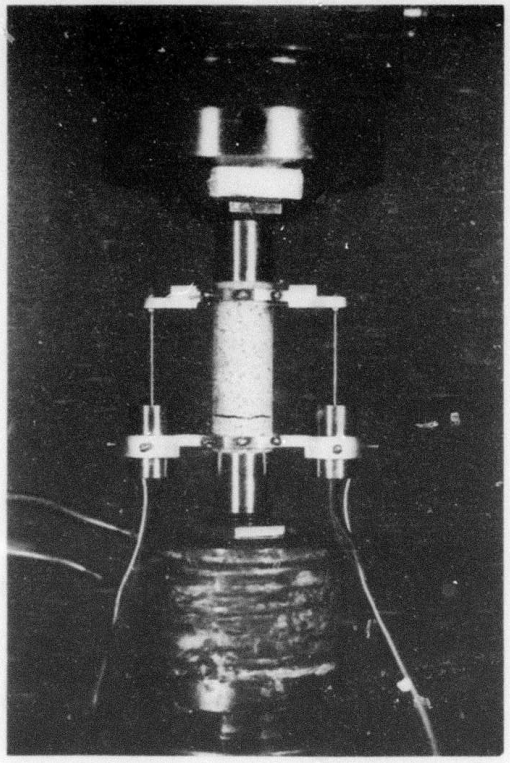

Fig. 1 Experimental set-up for uniaxial cyclic tension and tension-compression testing.

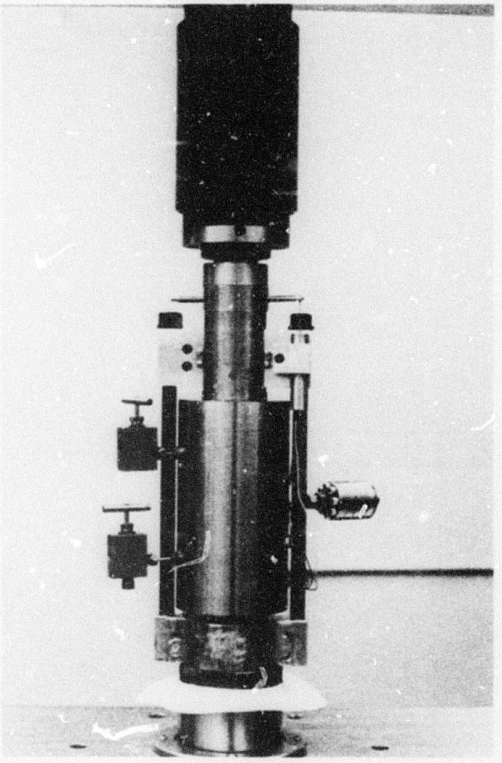

Fig. 2 Experimental set-up for triaxial cyclic compression testing.

The load from the specimen to the load cell is transmitted through the upper portion of the triaxial cell. Figure 3 is a detailed cross-section of the triaxial system. The variation of confining pressure with time has been monitored, and at 1,000 psi oil pressure it shows fluctuations of ± 30 psi per cycle while maintaining the mean pressure constant at 1,000 psi. At the present no further improvements are planned, but it is believed that the ± 3% fluctuations have only a very limited effect on the results.

A pressure generating system has been built on a mobile 2' x 3' table, consisting of an "Enerpac" hand pump for filling the cell, a 0-15,000 psi positive displacement pump for accurate pressurization, a 6" Heise gage, an accumulator whose purpose is to prevent variations in confining pressure when the specimen deforms, and other valves and accessories (Fig. 4). A BLH 0-20,000 psi pressure transducer is directly connected to the triaxial cell and provides accurate continuous pressure monitoring. The longitudinal displacement of loaded specimens is measured indirectly by two DCDT transducers mounted on the outside of the triaxial cell.

Experimental Program

The objectives of the experimental program have been to (a) determine the mechanical behavior of rock under cyclic loading and provide data that is both basic and useful in engineering practice, and (b) study the internal mechanism that brings about cyclic fatigue.

Four major types of cyclic loading were used in the reported period, namely uniaxial compression, triaxial compression, uniaxial tension and tension-compression. The details of the testing procedure in uniaxial compression and tension can be found in reference 1. The only difference between the uniaxial and the triaxial compression testing procedures was that in the latter, specimens were subjected to a static confining pressure while cycling the vertical load. The triaxial cell was so built that the removal of a failed specimen and the insertion of a new one could be done without removing the cell from its rigid connection to the loading machine hydraulic ram. Specimens were jacketed with heat shrinkable

LEGEND:

1. Load Cell
2. Load Cell Adaptor
3. Pressure Block
4. Extender
5. DCDT Transducer
6. Yoke Bar
7. Mounting Block
8. Yoke Rod
9. Compression Nut
10. Upper Nut
11. Upper Piston
12. Upper Platen
13. Oil Outlet Port
14. Rock Specimen
15. Pressure Transducer
16. Piston Attaching Screw
17. Ram Adaptor

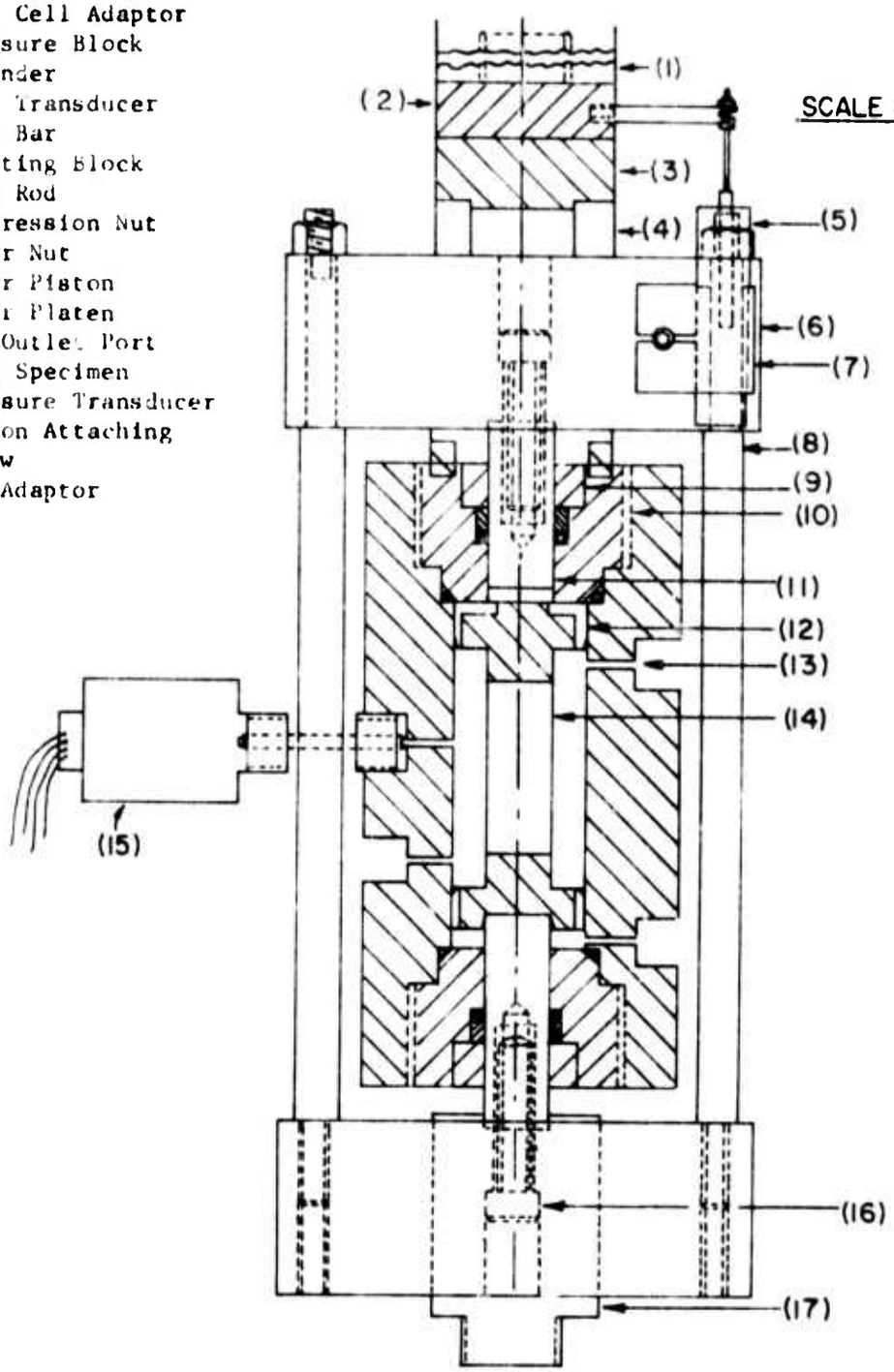

Fig. 3 FRONT VIEW OF THE TRIAXIAL CELL FOR FATIGUE TESTING

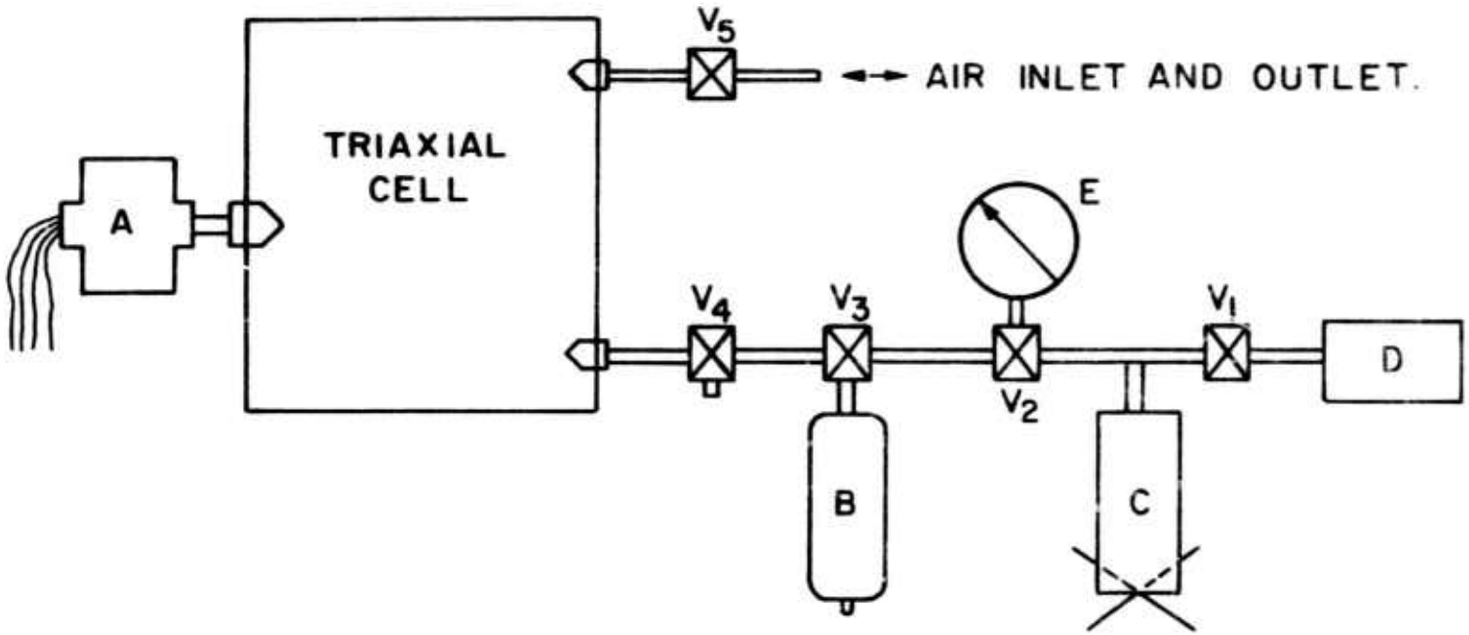

LEGEND

A - PRESSURE TRANSDUCER
B - ACCUMULATOR
C - PRESSURE GENERATOR
D - OIL PUMP
E - PRESSURE GAUGE
V_1 TO V_5 - VALVES

Fig. 4 Schematic diagram of the confining pressure generating system.

tubing and installed in the triaxial cell which was then sealed and brought into contact with the load cell. The free annulus in the cell was filled with hydraulic oil and pressurized to the desired level while keeping the vertical load at a magnitude equal or greater than that of the oil. The vertical cyclic loading was applied as described in the annual report. Strain monitoring was indirectly done through two DCDT transducers mounted on the outside of the cell (Fig. 3). The acoustic emission was detected by attaching the piezoelectric transducer (1) to the outside surface of the triaxial cell.

The testing procedure in uniaxial tension-compression tests was very similar to that used in uniaxial tension tests, except that the range of stresses applied during each cycle was not confined to tension only or compression only. In a series of tests the cyclic lower peak was barely taken into the compression zone. In another series of tests the stress range was kept constant at 10,000 psi while changing the peaks from test to test. In yet another series of tests the stress range was varied to include the critical zones of failure in both tension and compression. Details are given in the next chapter.

EXPERIMENTAL RESULTS

A - UNIAXIAL COMPRESSION

The two rocks tested under the present program, Berea sandstone and Westerly granite, were first loaded monotonically to determine their respective uniaxial compressive strengths at loading rates equivalent to "static" loading, 1 cps., 4 cps. In both rocks there was a substantial difference in strength between the "static" and the faster loadings (~20%) but no difference was observed between the two cyclic frequencies (Table 1).

Stress-Controlled Tests

In these tests the independent variable was the axial load. This load was programmed such that it followed a triangularly shaped cyclic function. The lower peak was kept constant throughout the program at about 200 psi, the upper peak was kept constant during a test but varied from test to test, when desired. The values first used for upper peak loads were those close to the monotonic compressive strength for the loading rate comparable to the cyclic frequency used. Thereafter, the upper peak values were lowered in steps of 5% or less until no failure was obtained in more than 10^6 cycles. The results are detailed in the following sections.

(a) S-N Characteristics

In the first annual report (1) it was shown that both Tennessee marble and Indiana limestone exhibited cyclic loading fatigue when loaded in stress control. To confirm the results two additional rock types were similarly tested under this year's program. Quantitative results in the form of S-N curves are given in Figs. 5 and 6. Both the sandstone and the granite exhibited fatigue behavior, i.e., they were weakened by repetitive loading. Within the limit set for these tests (10^6 cycles) the fatigue strength was as low as 55% in Berea sandstone and 60% in Westerly granite of the respective compressive strengths.

Although both rocks exhibited a definite weakening due to cyclic loading, their S-N relationship was quite different. In the sandstone a

TABLE 1

COMPRESSIVE STRENGTHS AT DIFFERENT LOADING RATES

Rock	Specimens Tested	Loading Rate (psi/sec)	Equivalent Cyclic Frequency (psi)	Mean Comp. Strength (psi)
Berea Sandstone	10	100	"static"	10, 400
	8	25, 760	1	12, 800
	6	103, 040	4	12, 800
Westerly Granite	3	200	"static"	38, 200
	4	93, 000	1	46, 500
	4	372, 000	4	46, 500

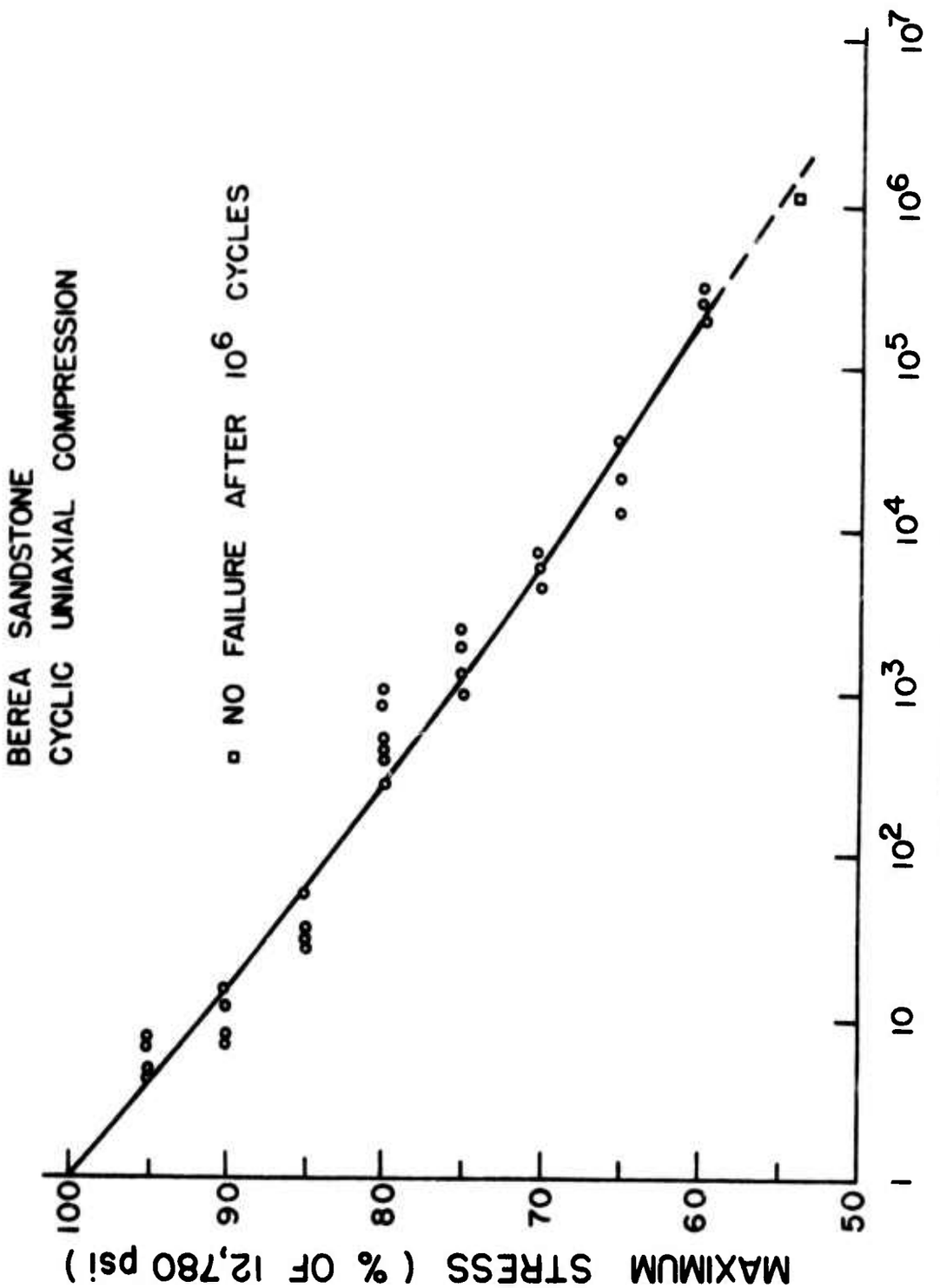

Fig. 5 S-N characteristics in uniaxial compression--Berea sandstone.

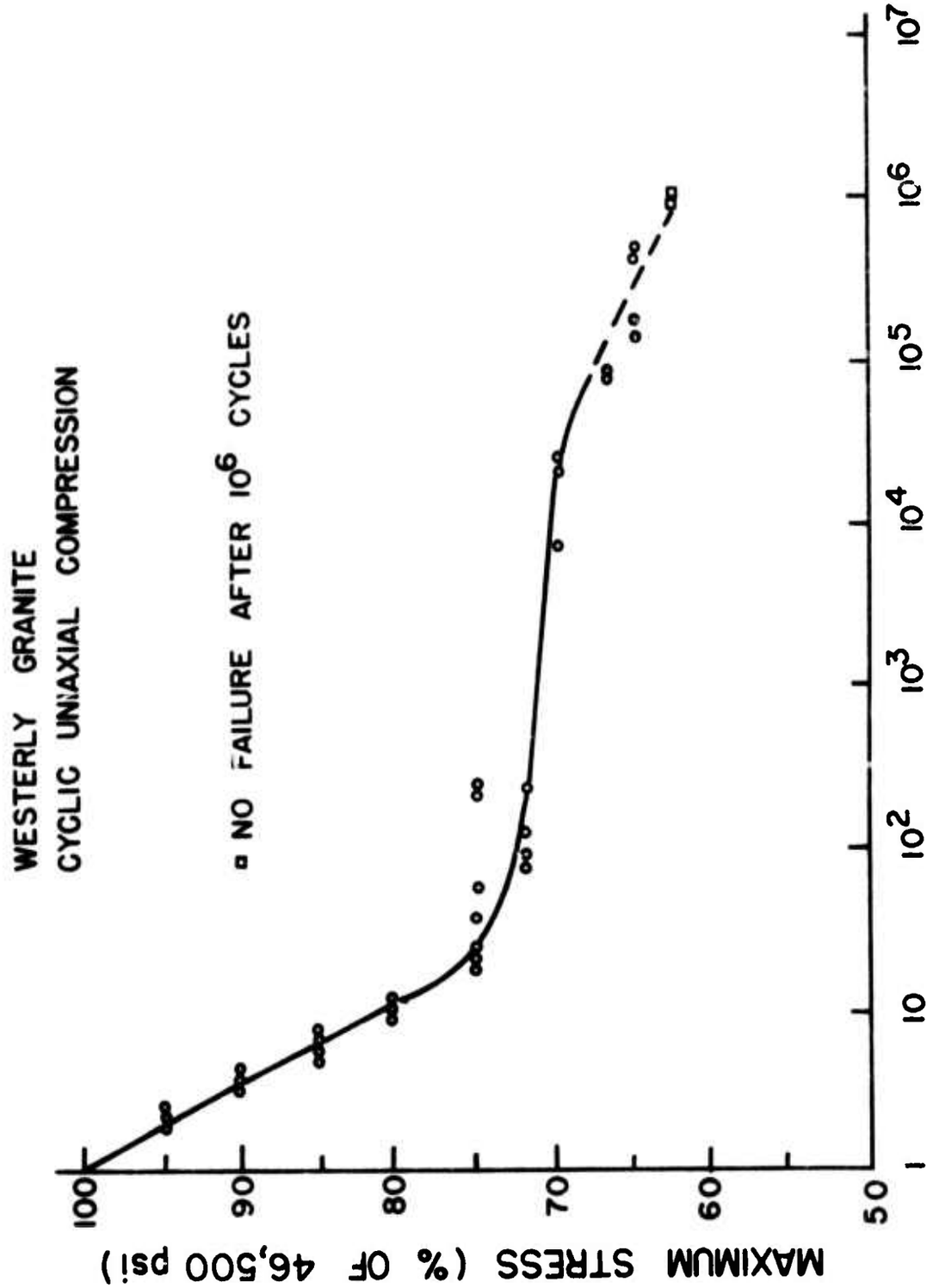

Fig. 6 S-N characteristics in uniaxial compression--Westerly granite.

linear relationship seems to prevail (Fig. 5), while the best fitting curve for the granite could be divided into three linear portions exhibiting a sharp drop in strength with cycling in the upper 25%, followed by a drastic strengthening and increased resistance to fatigue in the next 5% and then again a rather sharp drop in the remaining 10% (Fig. 6). A tempting speculation regarding the granite S-N curve is that it could be related to the complete stress-strain curve for the rock (3). In the post-failure zone this curve is unstable and has a positive slope in its upper quarter, followed by a negative slope for a small portion of stress and continued again by a positive slope (Fig. 7). The extent of the top portion of the descending complete stress-strain curve may coincide with the top range of the S-N curve (for which less than 100 cycles are sufficient to bring about failure). Similarly, the next two portions of the complete stress-strain curve appear to coincide with the continuation of the S-N curve. The implication suggested is that the extent of permanent strain exhibited by the complete stress-strain curve controls the fatigue life at different levels of maximum stress.

In an attempt to verify whether any correlation can be found between S-N curves and the appropriate complete stress-strain behavior in all of the rocks tested under this program, the summarizing plots shown in Fig. 8 were obtained. By comparing the top 25% of the stress range a direct correlation between the slope of the descending stress-strain curve and that of the S-N curve is noticed. The gentler the descending portion of the stress-strain curve the less affected by fatigue loading is the rock. Since the slope delineates the amount of permissible strain for each stress level, the above results could also indicate a correlation between that strain and fatigue life.

Quantitatively, the best fit curve for the experimental S-N points in Berea sandstone is given by

$$S = 100 - 20 \log N \qquad 1<N<10^6$$

In Westerly granite three linear relationships can be distinguished:

$$S = 100 - 20 \log N \qquad 1<N<20$$
$$S = 75 - \log N \qquad 20<N<2\times10^4$$
$$S = 95 - 5 \log N \qquad 2\times10^4<N<10^6$$

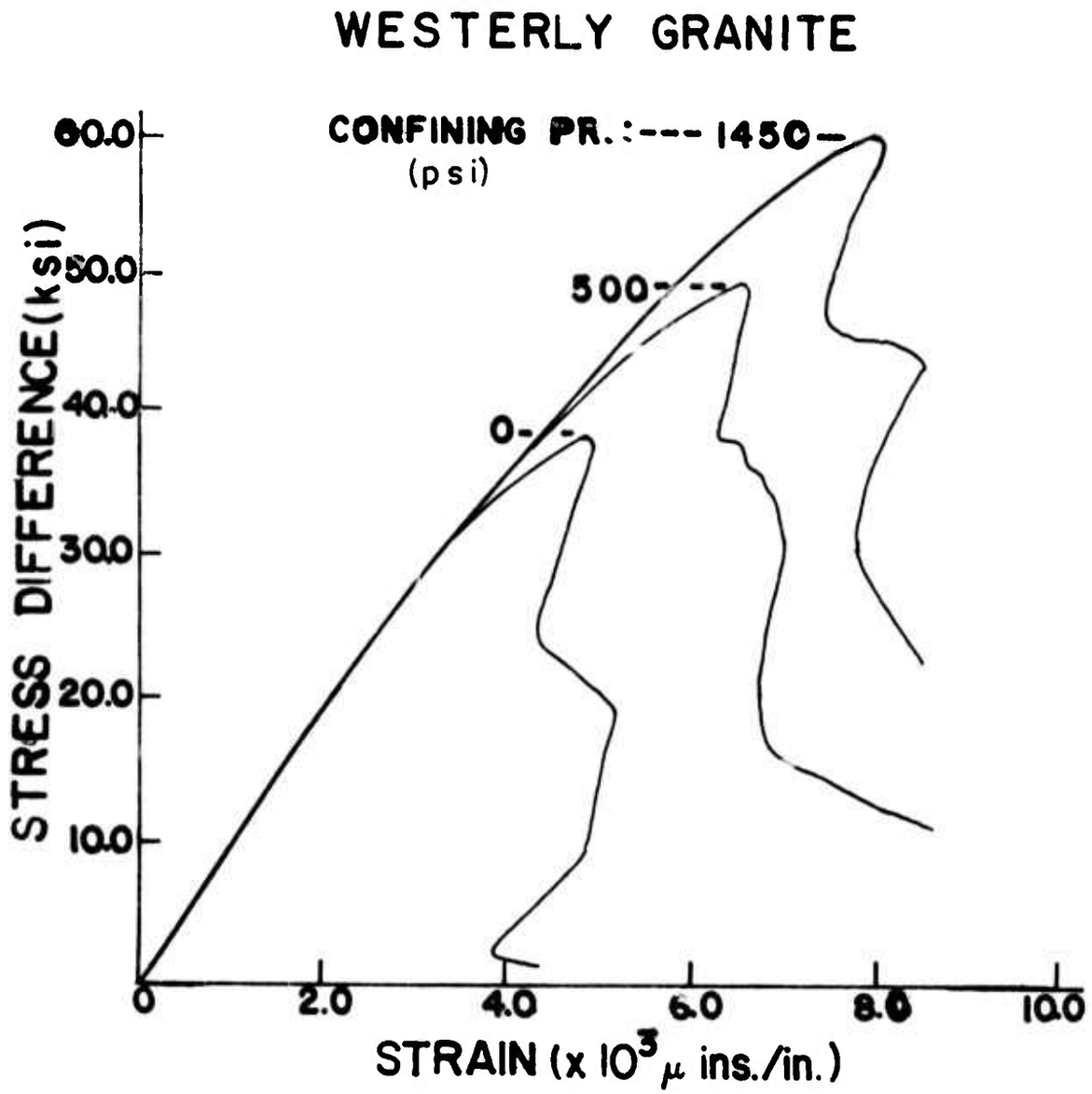

Fig. 7 Complete stress-strain curves for Westerly granite (after Wawersik and Brace).

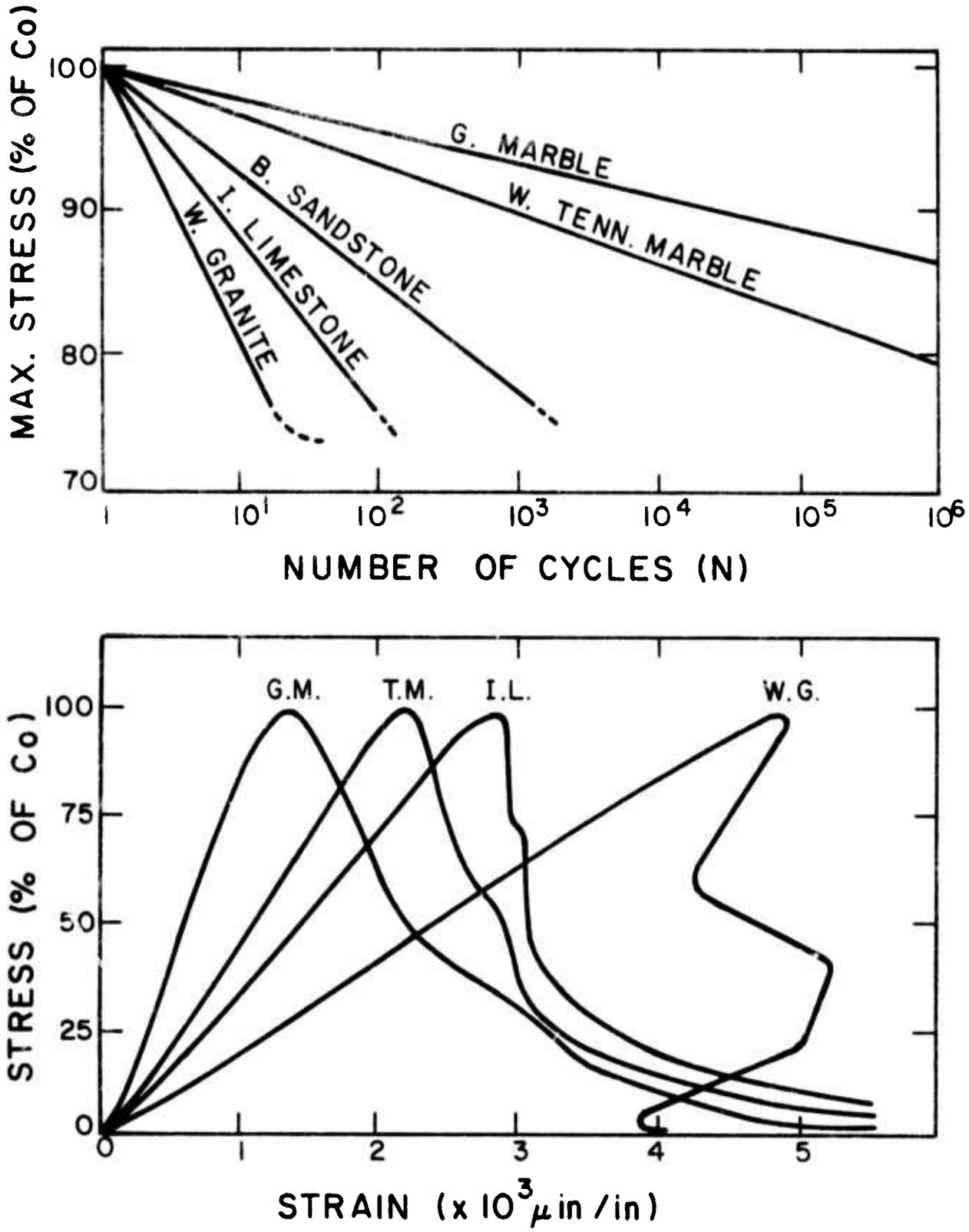

Fig. 8 Comparison between the fatigue life of rocks tested under the reported program and the slope of the descending part of their respective complete stress-strain curves.

A practical application derived from the S-N results obtained is that in designing hard intact rock structures the fatigue strength at 10^6 cycles, conservatively taken as one half of the measured static compressive strength (Table 2), would provide protection not only against static and dynamic compressive loads but also against cyclic compressive stresses such as encountered in earthquakes, blasting, etc.

(b) Cyclic Stress-Strain, Strain-Time and Acoustic Emission

The basic cyclic stress-strain behavior was not different from that observed in previously tested rocks (1). Three stages (primary, steady state, tertiary) could always be identified in tests longer than 10 cycles. The first cycle invariably yielded the largest hysteresis due probably to permanent closing of existing openings and cracks and initiation of microfractures. As a result of the reduced porosity, the hysteresis in the granite was, however, very low as compared to the sandstone. Figures 9 and 10 show typical plots of stress-strain, strain-time and cumulative acoustic emission-time in both tested rocks. As in the previously reported tests both strain-time and acoustic emission-time were indicative of the three stages undergone by cyclically compressed specimens. In particular, it is noted that the acoustic emission accelerates considerably in the third or final stage, probably as a result of the propagation and coalescence of microcracks prior to failure. The warning received by the sharp increase in "noise" could be utilized in practice to alert that fatigue failure is imminent.

The amount of strain difference between the upper peaks of the last and first cycles (the cyclic creep), was measured and the average values were plotted in Figs. 11 and 12. Comparing the granite results with the complete stress-strain curves of an identical rock type as obtained by Wawersik and Brace (3), it is noticed that in accord with the two previously tested rocks (1), the cyclic creep at different levels of $\underline{S}$ is bounded by the ascending and descending portions of the stress-strain curve. In particular, the Class II character of Westerly granite is apparent in Fig. 12.

Lateral strain was measured in selected specimens and typical recordings are shown in Figs. 13 and 14. The three stages of deformation are again noticeable, with the exception that both the cyclic creep of

TABLE 2

COMPRESSIVE AND FATIGUE STRENGTHS OF FOUR TESTED ROCKS

Rock Type	Static Compressive Strength (psi)	Fatigue Strength (10^6 Cycles) (psi)	$\frac{\text{Fatigue Strength}}{\text{Static Compressive Strength}}$ (%)
White Tennessee Marble*	21, 150	17, 500	83
Indiana Limestone*	9, 500	6, 470	68
Berea Sandstone	10, 400	7, 070	68
Western Granite	38, 200	27, 850	73

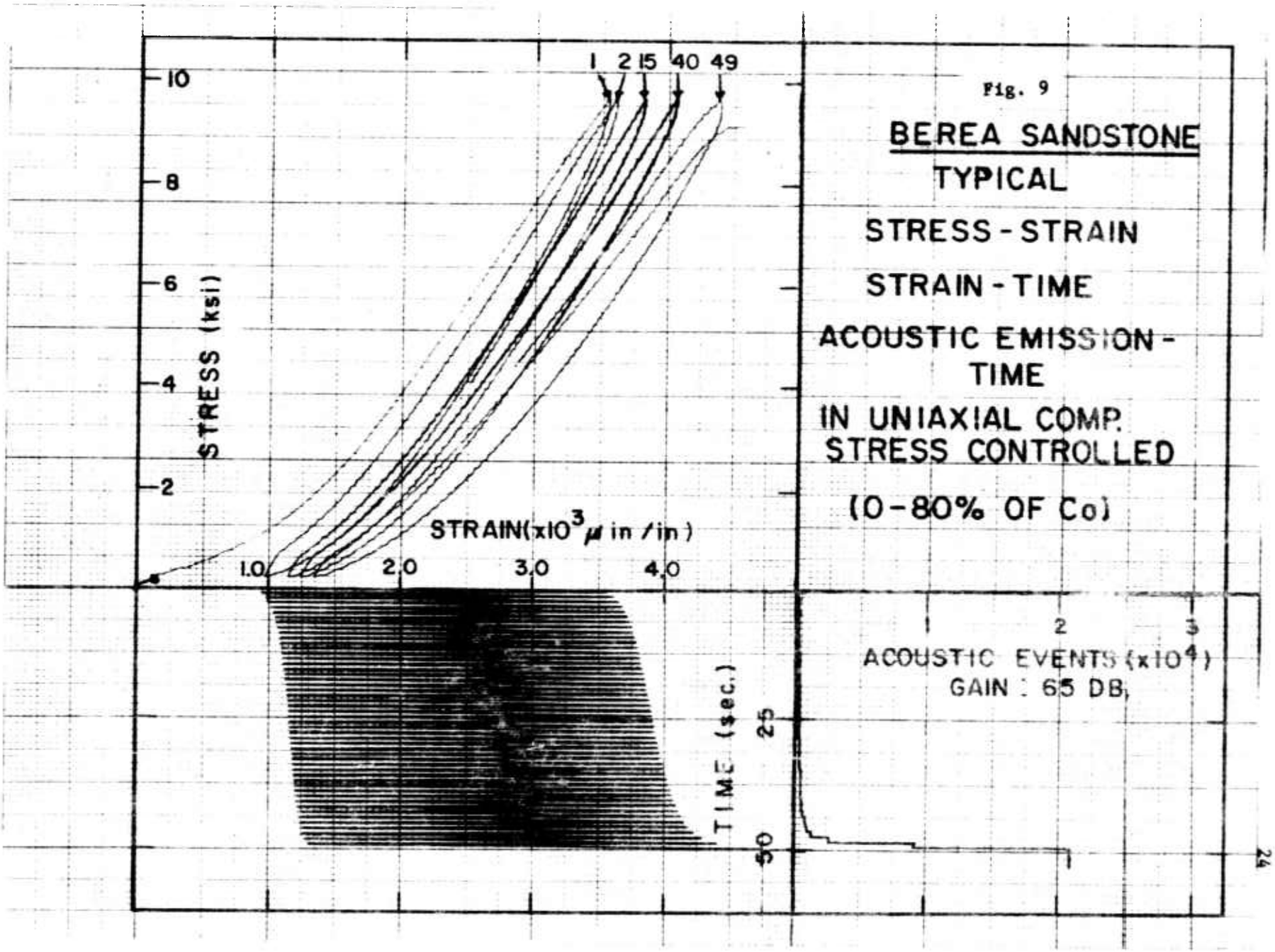

Fig. 9

BEREA SANDSTONE

TYPICAL

STRESS - STRAIN

STRAIN - TIME

ACOUSTIC EMISSION - TIME

IN UNIAXIAL COMP. STRESS CONTROLLED

(0 - 80% OF Co)

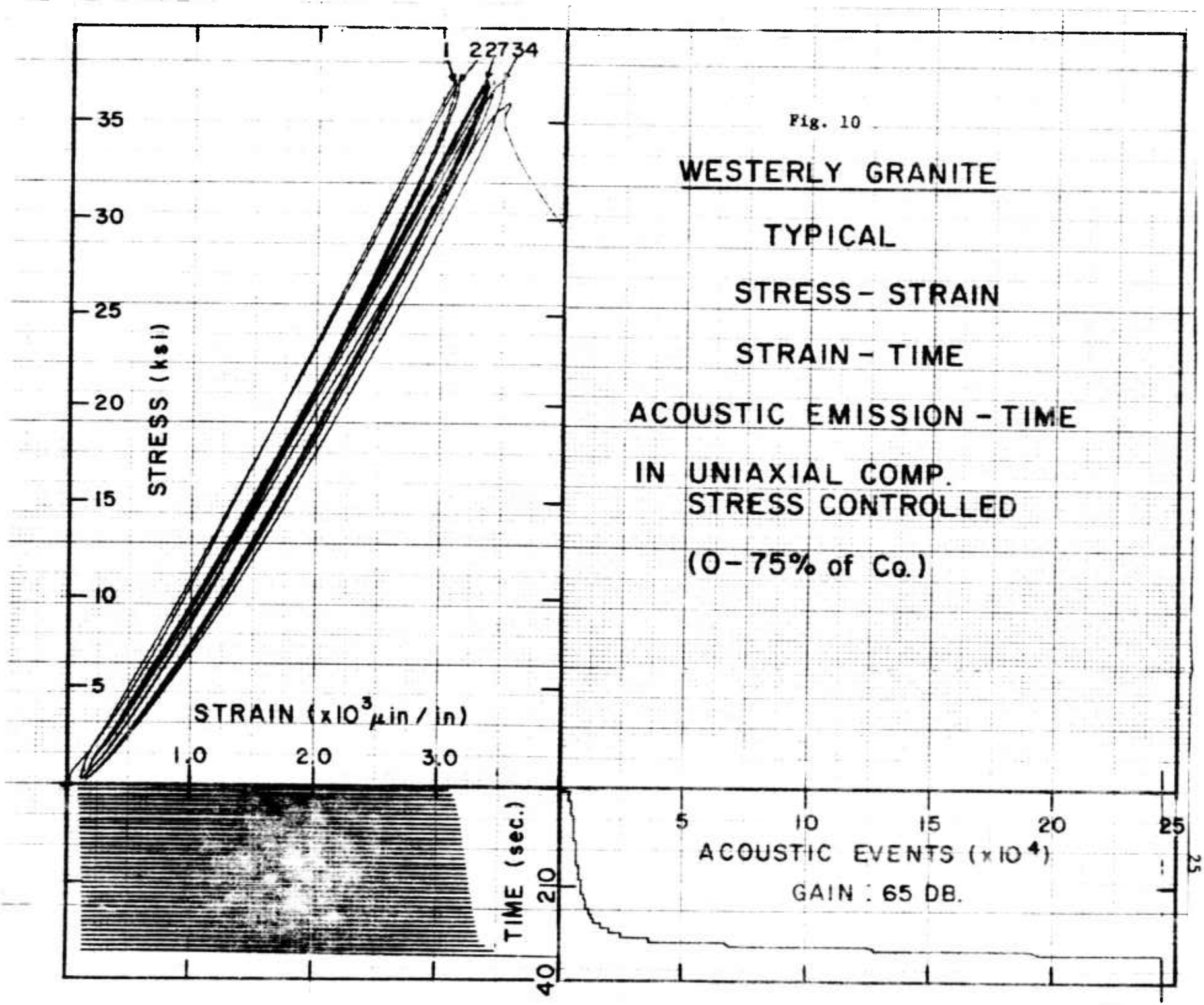

Fig. 10

WESTERLY GRANITE

TYPICAL

STRESS - STRAIN

STRAIN - TIME

ACOUSTIC EMISSION - TIME

IN UNIAXIAL COMP.
STRESS CONTROLLED

(0 - 75% of Co.)

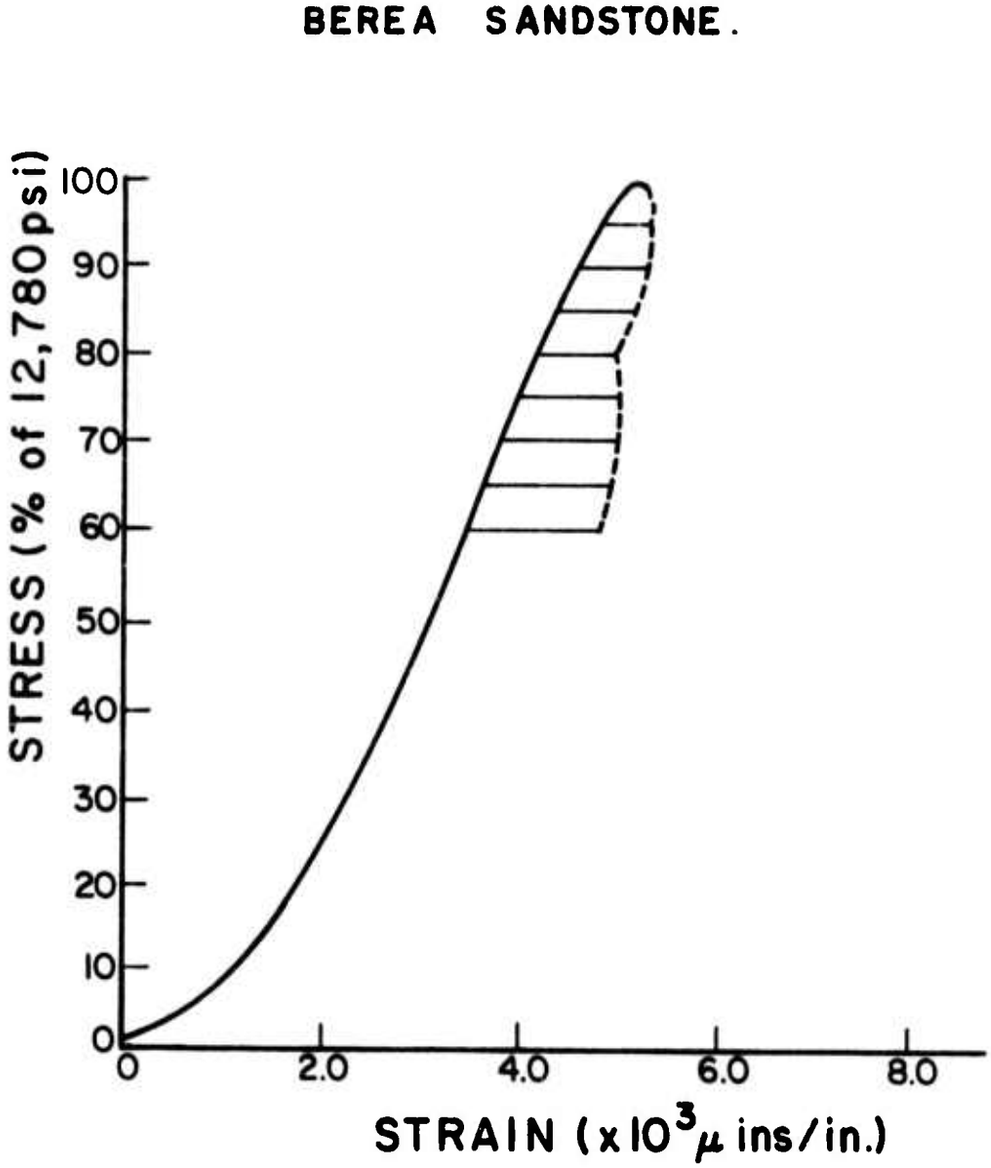

Fig. 11 Upper peak cyclic creep for different stress levels--Berea sandstone.

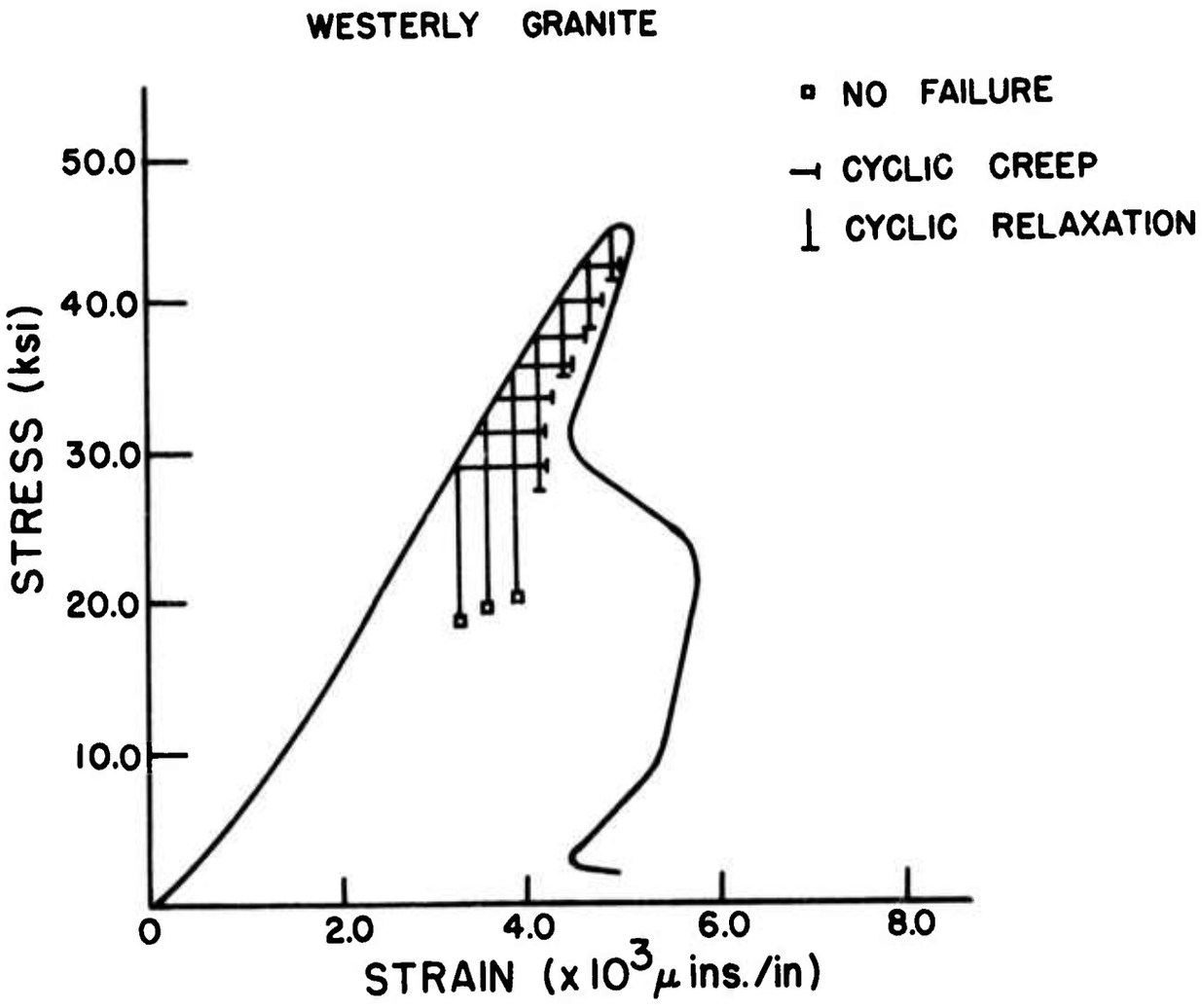

Fig. 12 Upper peak cyclic creep and cyclic stress relaxation at different levels of stress and strain respectively versus the complete stress-strain curve--Westerly granite.

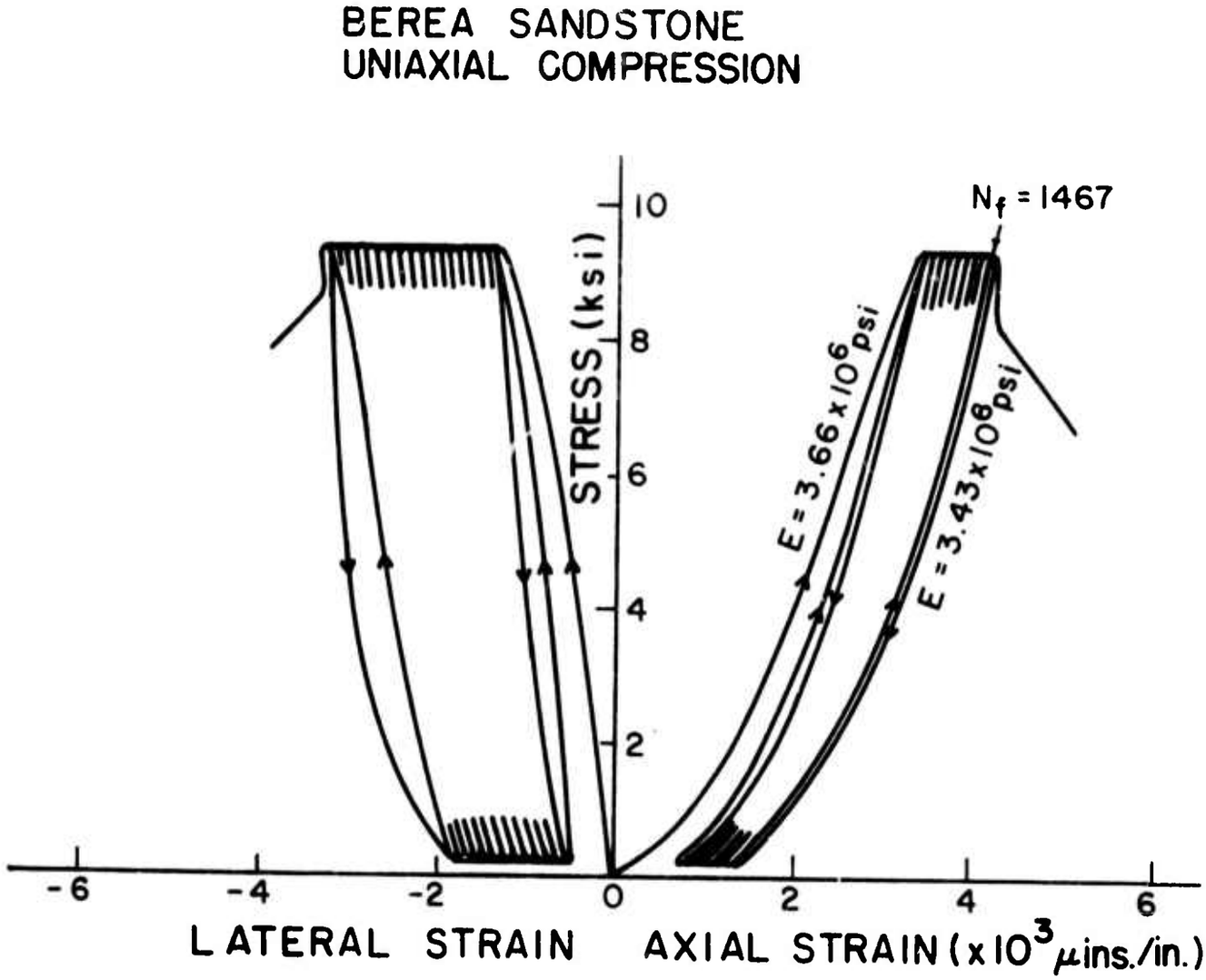

Fig. 13 Typical stress vs. lateral and axial strain curves in stress controlled cyclic uniaxial compression--Berea sandstone.

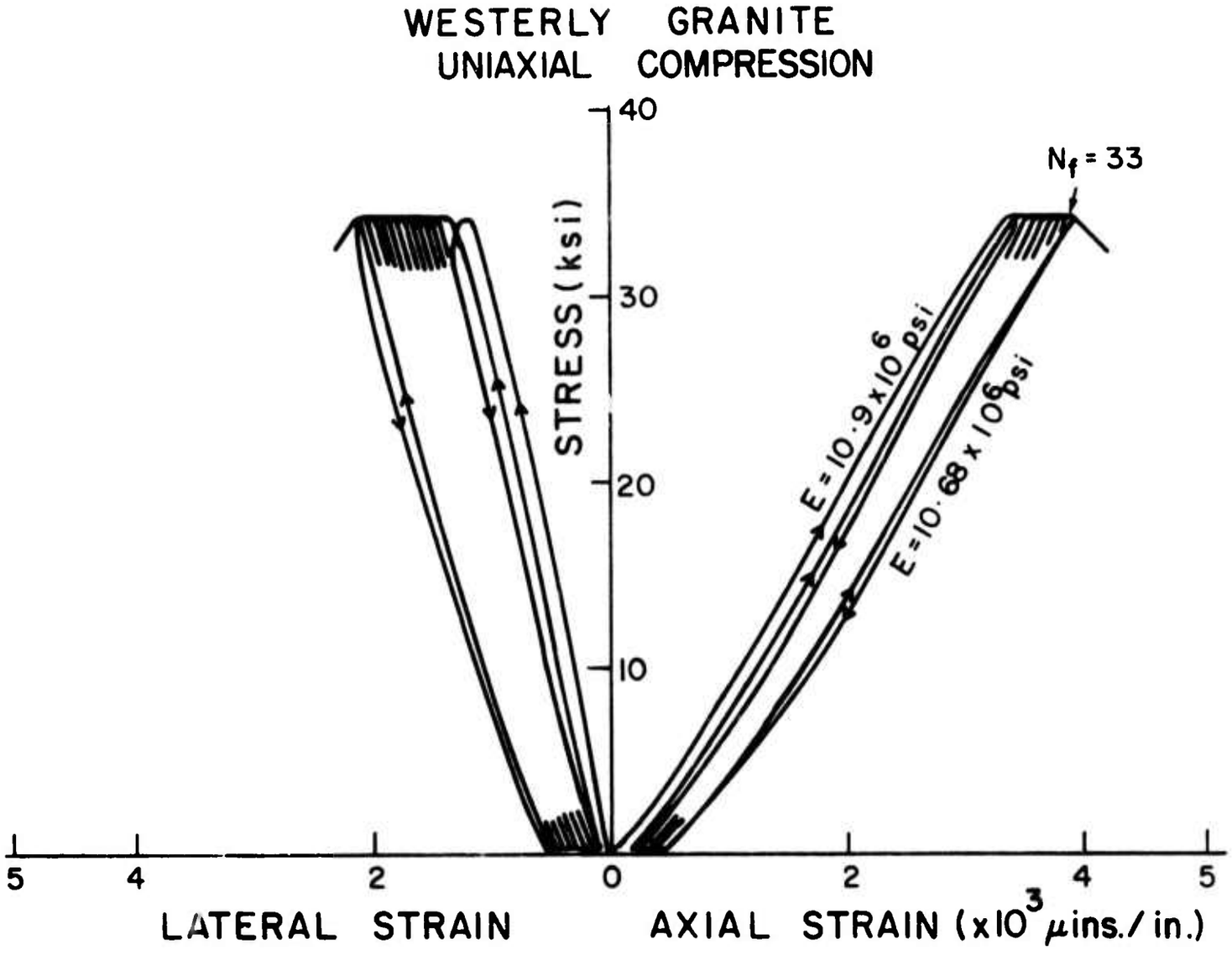

Fig. 14 Typical stress vs. lateral and axial strain curves in stress controlled cyclic uniaxial compression--Westerly granite.

the upper peak and the permanent strain at the lower peak are considerably larger than in the axial direction. Typical Poisson's ratio values varied from 0.28 in the first cycle to 0.44 in the last cycle in Westerly granite, and from 0.21 to 0.48 in Berea sandstone. These values were taken at 50% of the upper peak stress.

From longitudinal and lateral strain measurements the volumetric strain was calculated and plotted against applied stress (Figs. 15 and 16). Although Westerly granite shows considerably more resistance than Berea sandstone, both rocks develop during cycling negative volumetric changes contrary to theoretical expectations from elastic materials. This "cyclic dilatancy" was previously found in the tested marble and limestone (1).

Stress Controlled Tests with Variable Upper Peaks

An attempt was made to study the loading path dependence in stress controlled tests. While keeping the lower peak constant, the upper peak stress was varied during the test and the number of cycles, as well as the total cyclic creep, were monitored. As shown in Figs. 17 and 18 the total amount of permanent strain at the upper peak level at which a specimen failed was consistently unaffected by the previous magnitudes of the upper peak. Whether the upper peak load was stepped up or stepped down, the total cyclic creep remained path independent. The consistency of this result was rather surprising. It is a further indication that the amount of upper peak level permanent strain actually controls fatigue failure. As has been stated above, it appears that the complete stress-strain curve provides the range for the maximum allowable deformation. This range is not path dependent as long as the path is within the complete stress-strain curve.

Stepping up or down the upper peak load during a test drastically affects the number of cycles to failure. Typical examples are shown in Figs. 17 and 18. Considerably more tests are needed to quantitatively determine the path dependency of fatigue life.

Stress-Controlled Tests of Failed Granite

The discovery of the complete stress-strain curve in recent years has changed the meaning of rock strength. The classical approach had

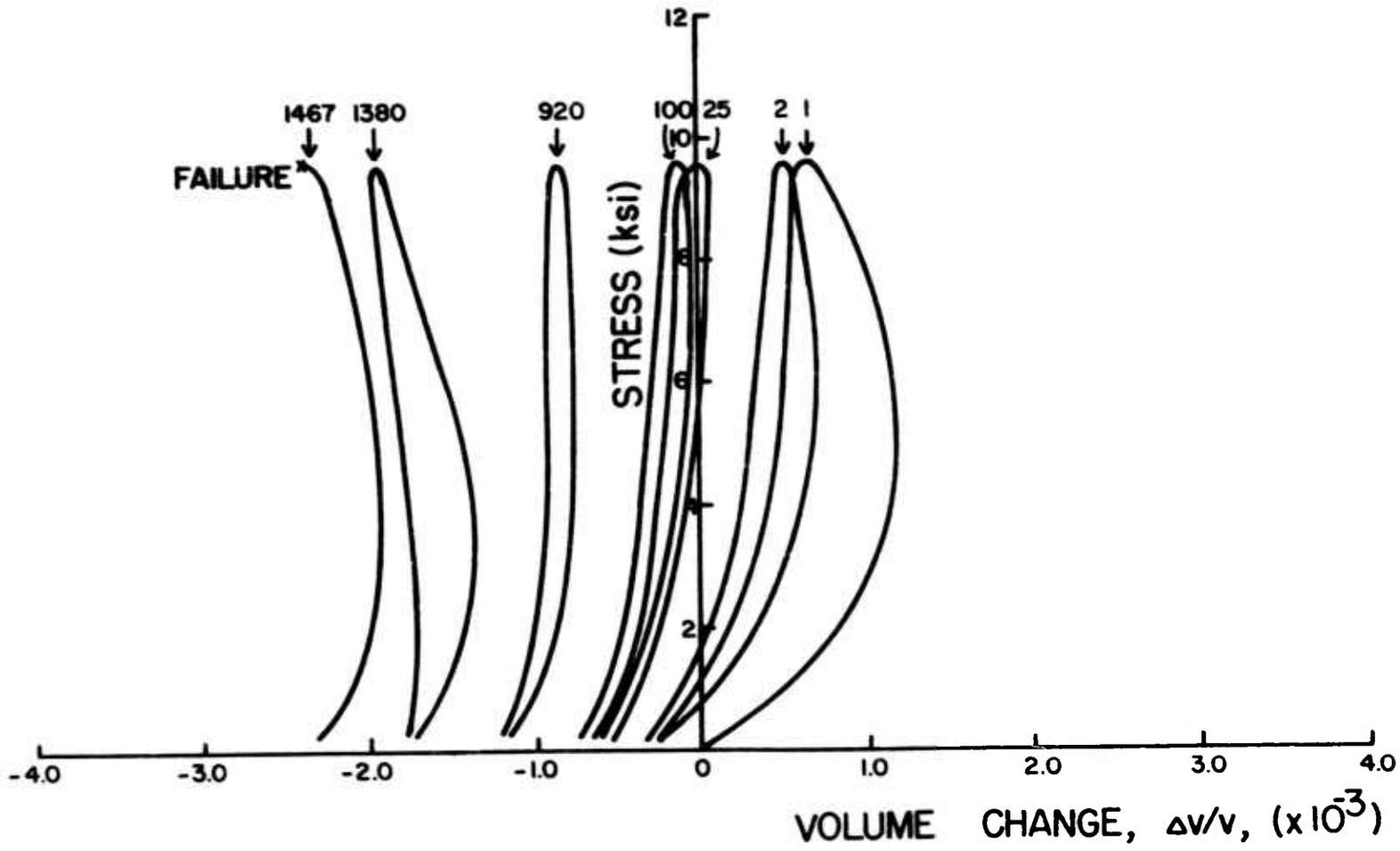

Fig. 15 Calculated typical volumetric changes--Berea sandstone.

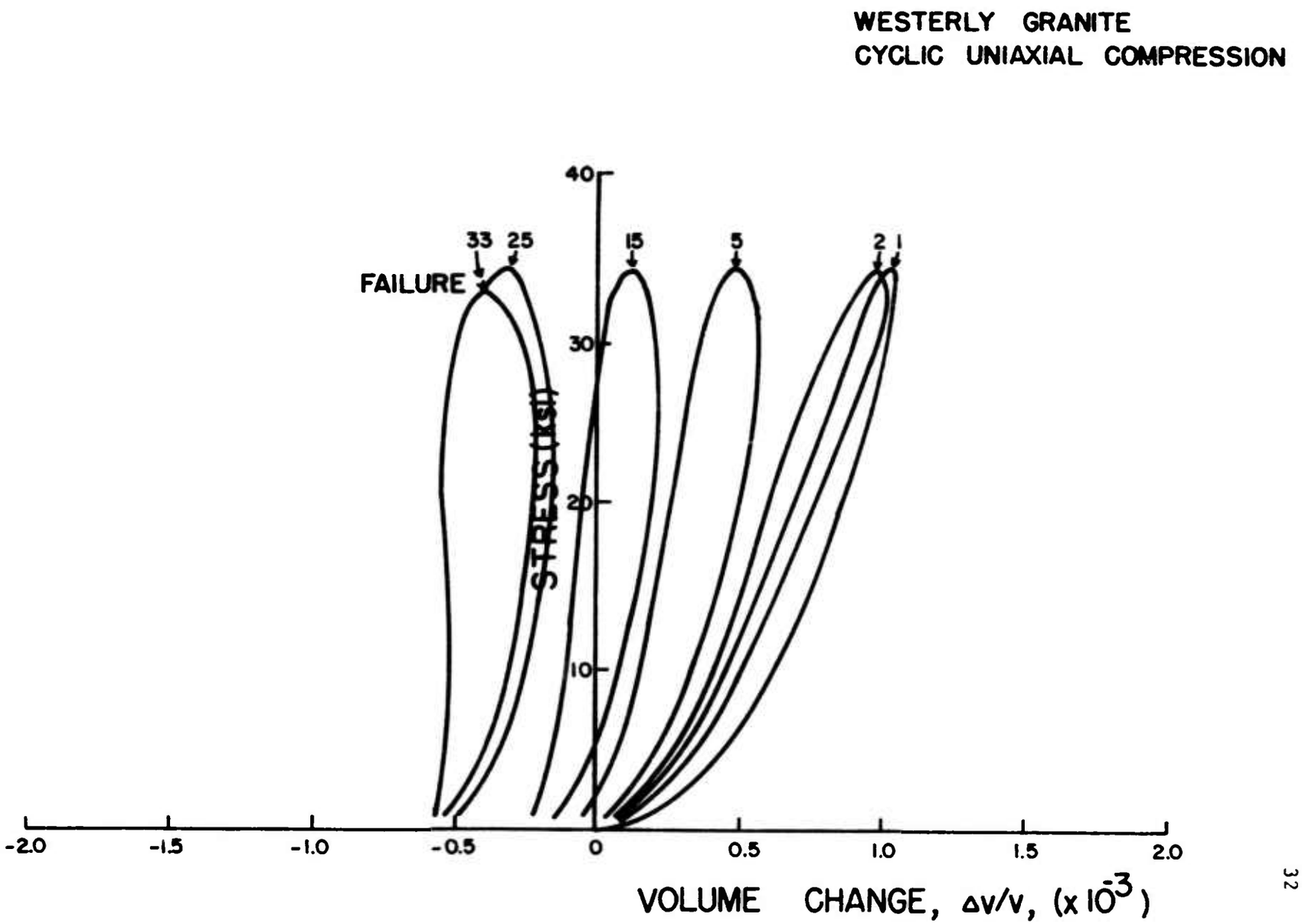

Fig. 16. Calculated typical volumetric changes--Westerly granite.

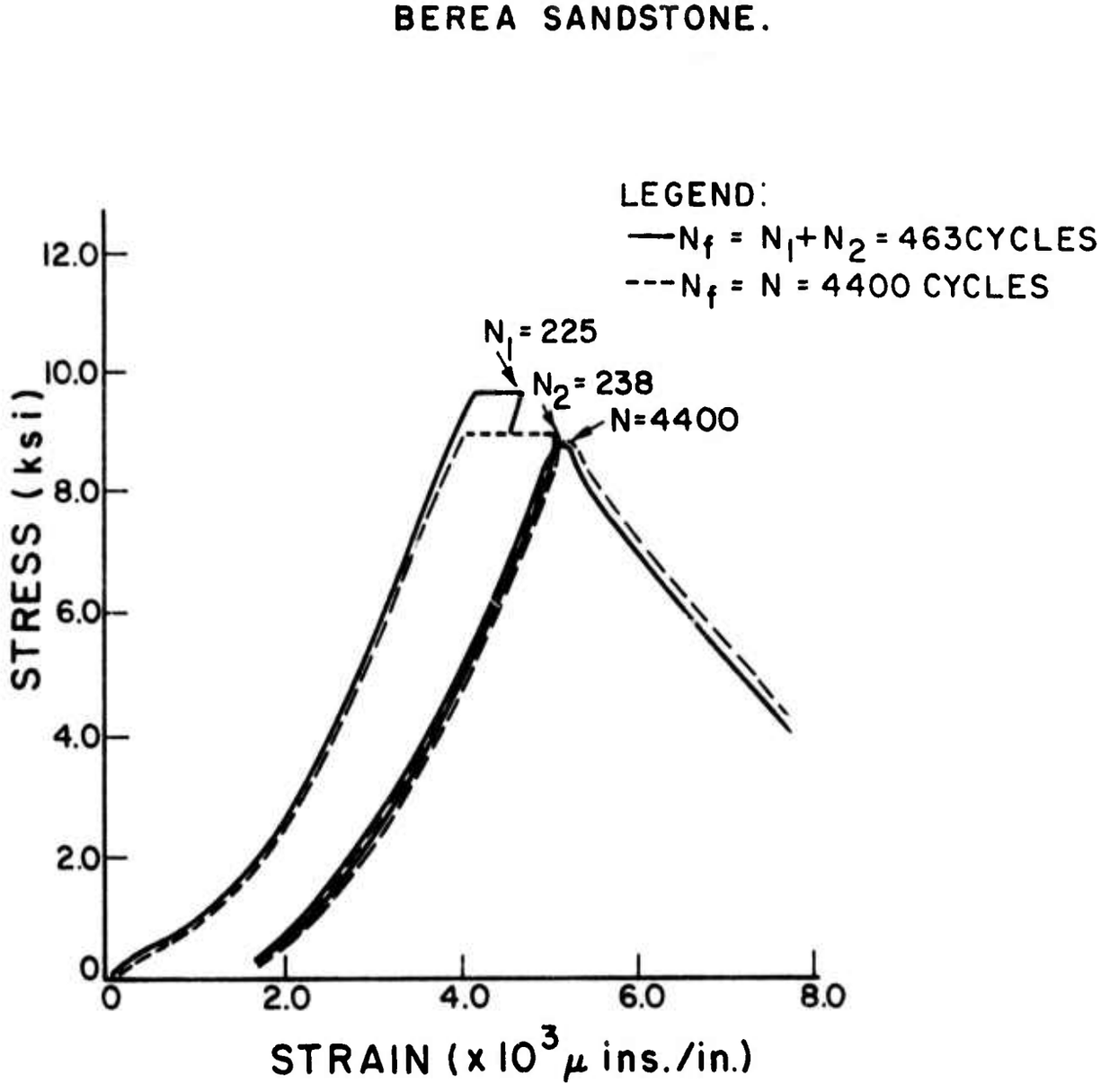

Fig. 17 Path dependence in stress controlled cyclic compression tests--Berea sandstone.

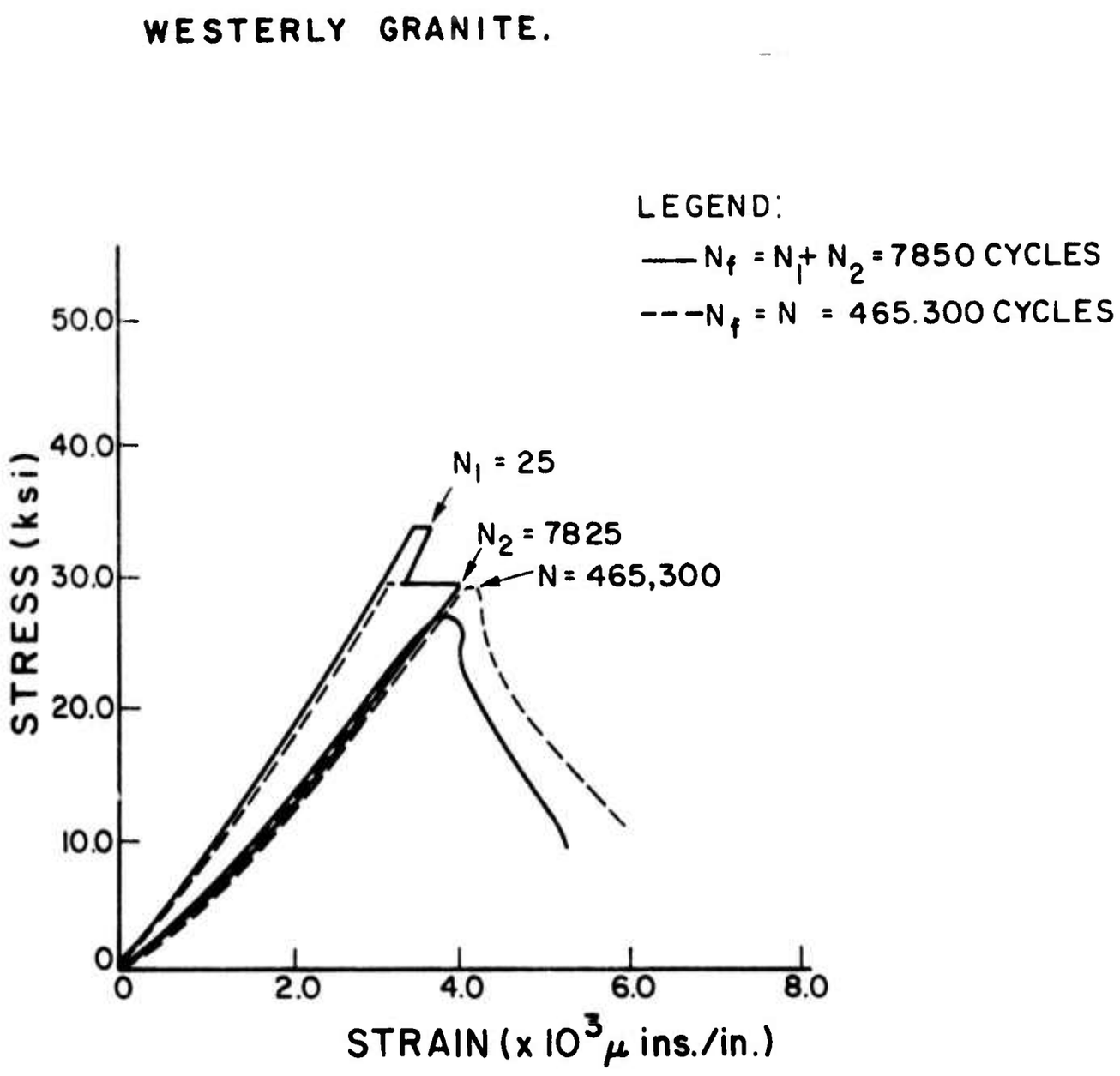

Fig. 18 Path dependence in stress controlled cyclic compression tests--Westerly granite.

that rock subjected to loads equal or larger than its compressive strength. would collapse violently and its load carrying ability eliminated. It has been demonstrated, however, (4) that under some conditions (like stiff machine loading, or strain-controlled loading) rock is capable of supporting substantial stresses even after it has reached its compressive strength. Such "failed" but active rock can be encountered in underground excavations, in pillars, sidewalls, etc. It was thus decided to test the ability of failed rock to support cyclic loading.

Two failed marbles were tested last year and the results were reported elsewhere (1). In the present program specimens of Westerly granite and Berea sandstone were loaded in strain-control to their compressive strength value, unloaded, and then cyclically loaded in stress control keeping the lower peak stress constant throughout the testing program. The S-N curves of failed rock are shown in Figs. 19 and 20. In Westerly granite the curve shows no significant reduction in fatigue strength as compared with that of unprefailed rock (Fig. 6), and averages a 5% weakening. This surprising result shows that the granite, although it had been loaded to a level equal to its compressive strength, still preserved most of its fatigue resistance. In Berea sandstone, however, a considerable reduction in fatigue strength is observed in the short life range (20% at 1 cycle). This reduction is almost completely diminished at 10^5 cycles. In general, testing of the two rock types shows that rock which had been loaded to its compressive strength value in strain control, although somehow weaker, has not lost its resistance to cyclic fatigue. In fact, at some levels of upper peak stress the fatigue strength of "failed" rock is hardly distinguishable from that of unpreloaded rock.

Strain-Controlled Tests

An extensive series of tests was run in both rocks under strain control (at 1 cps). The lower peak strain was kept constant at 480 μin/in throughout the program and the upper peak strain was varied from test to test. The value of the lower peak was chosen so that although it was relatively small it allowed the lower peak stress to relax during cycling without reaching zero stress, in which case the specimen would have lost contact with the loading platens. As in the stress-controlled tests, the

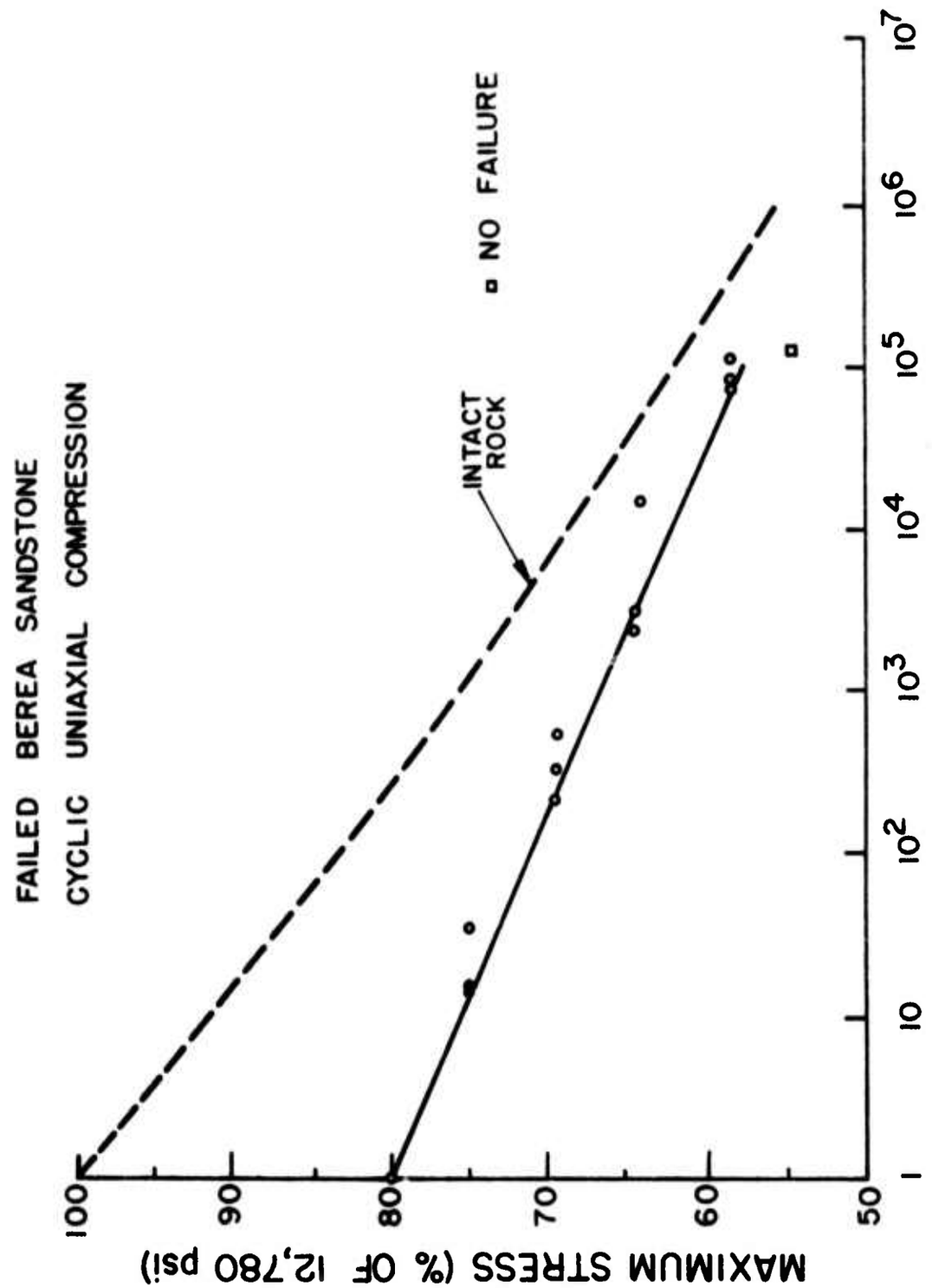

Fig. 19 S-N characteristics in uniaxial compression--failed Berea sandstone.

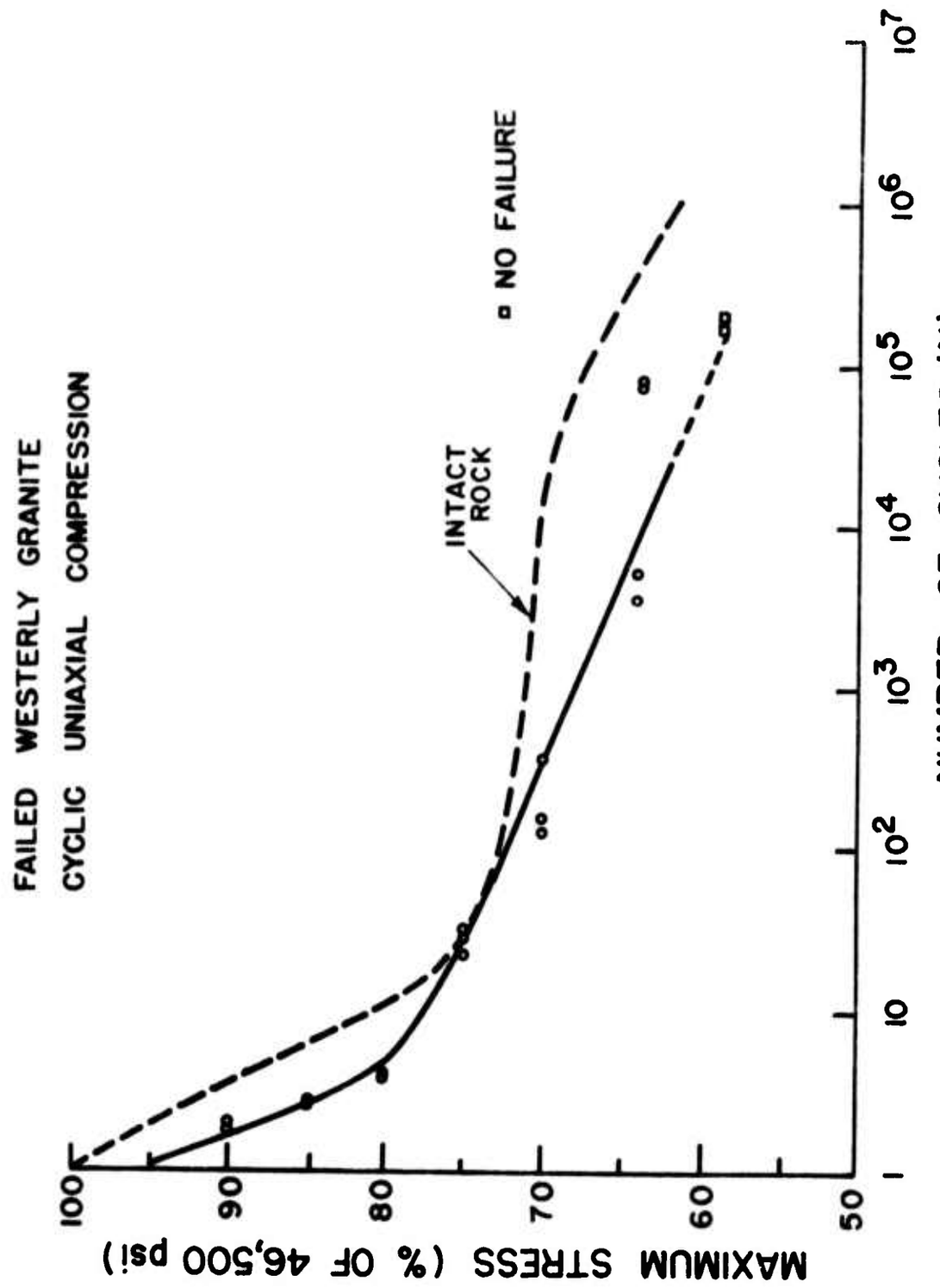

Fig. 20 S-N characteristics in uniaxial compression--failed Westerly granite.

number of cycles necessary to fatigue the rocks increased with the lowering of the upper peak strain. Fatigue life versus maximum applied cyclic strain was plotted for both rocks (Figs. 21 and 22) in the form of E-N curves.

The type of strain-controlled fatigue failure was significantly different from that encountered in stress controlled tests. In Berea sandstone failure was always slow, characterized by crumbling at the outside surface through a process similar to spalling. Continuous crumbling rapidly reduced the amount of peak stress and accelerated the cyclic stress relaxation (Fig. 23a). In some cases the specimens eventually failed, or were considered failed when the amount of crumbling became excessive; in others they reached a kind of equilibrium that appeared to require for fatigue failure many more cycles than the 10^5 limit (Fig. 24). In Westerly granite the type of failure depended on the range of upper peak strain. In the 90-100% range fatigue failure occurred violently within a few cycles (Fig. 22) and with limited cyclic stress relaxation (Figs. 23B and 25). In the 75-90% range failure was considerably slower, and was considered complete when chipping occurred at the surface. The relaxation was dominated by a steady-state stage (Fig. 23c), and later the amount of stress drop increased (Fig. 25). At 70% and lower the fatigue process seemed to cease and no failure was obtained within more than 10^5 cycles, although considerable relaxation was observed.

The type of failure and the amount of stress relaxation to failure could both be related to the complete stress-strain curve. Using the curve for Westerly granite (Fig. 12) one can easily establish that in a strain controlled cyclic test, with the upper peak in the top 10-15% of the ascending curve, a relatively small amount of stress relaxation will cause the cyclic stress-strain curve to intersect the descending positively sloped section of the complete stress-strain curve. Additional cycling will carry the relaxation to the outside of the curve thus causing a violent failure. When the process of fatigue failure is slow and seemingly endless, in both granite and sandstone, it is probably due to the need for the upper peak stress to reach the zero value before complete collapse. This is the case when the cyclic stress-strain curve does not intersect the descending part of the complete stress-strain curve. Figure 12 shows the average recorded cyclic creep of upper peak strains and the

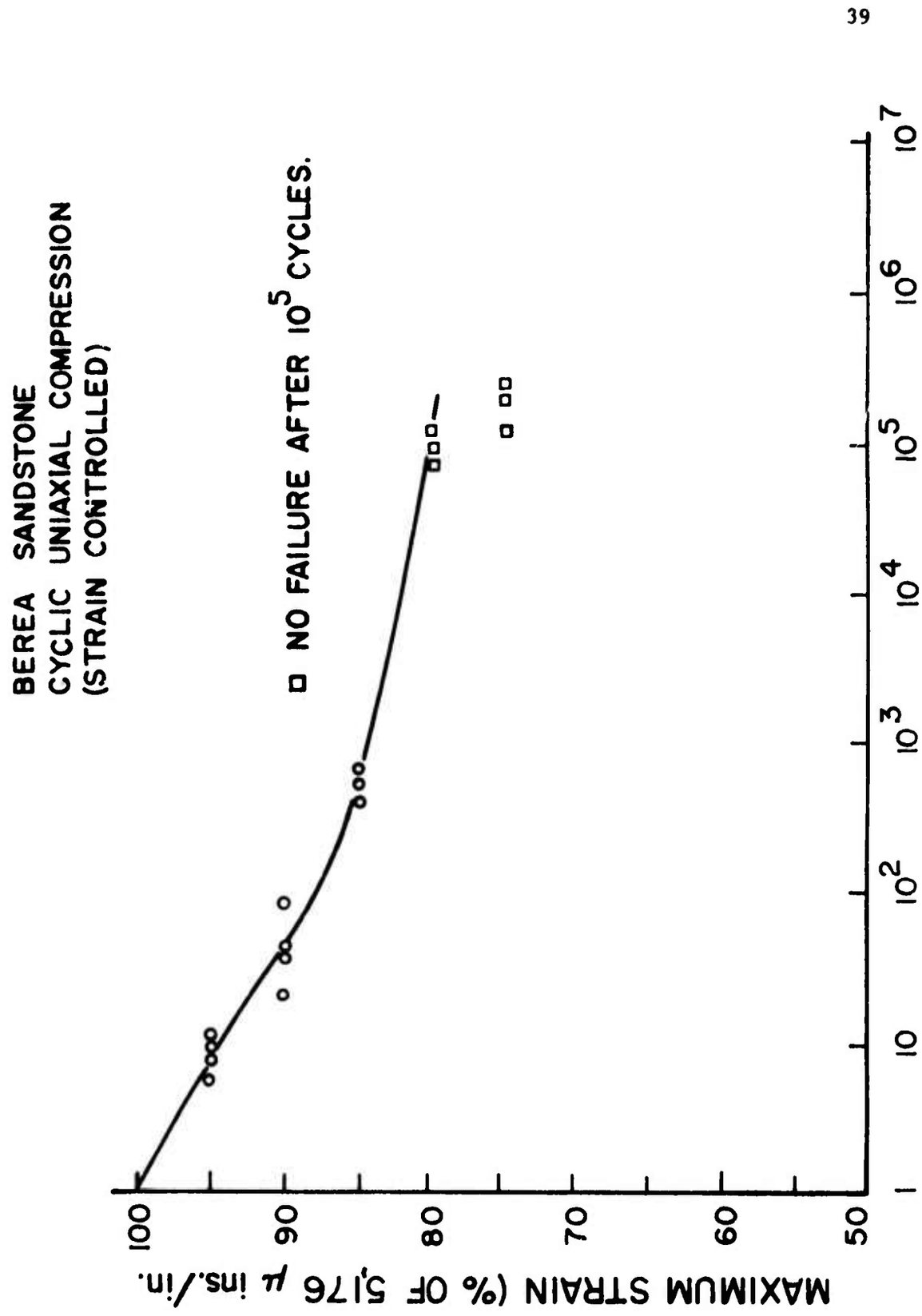

Fig. 21 E-N characteristics in uniaxial compression--Berea sandstone.

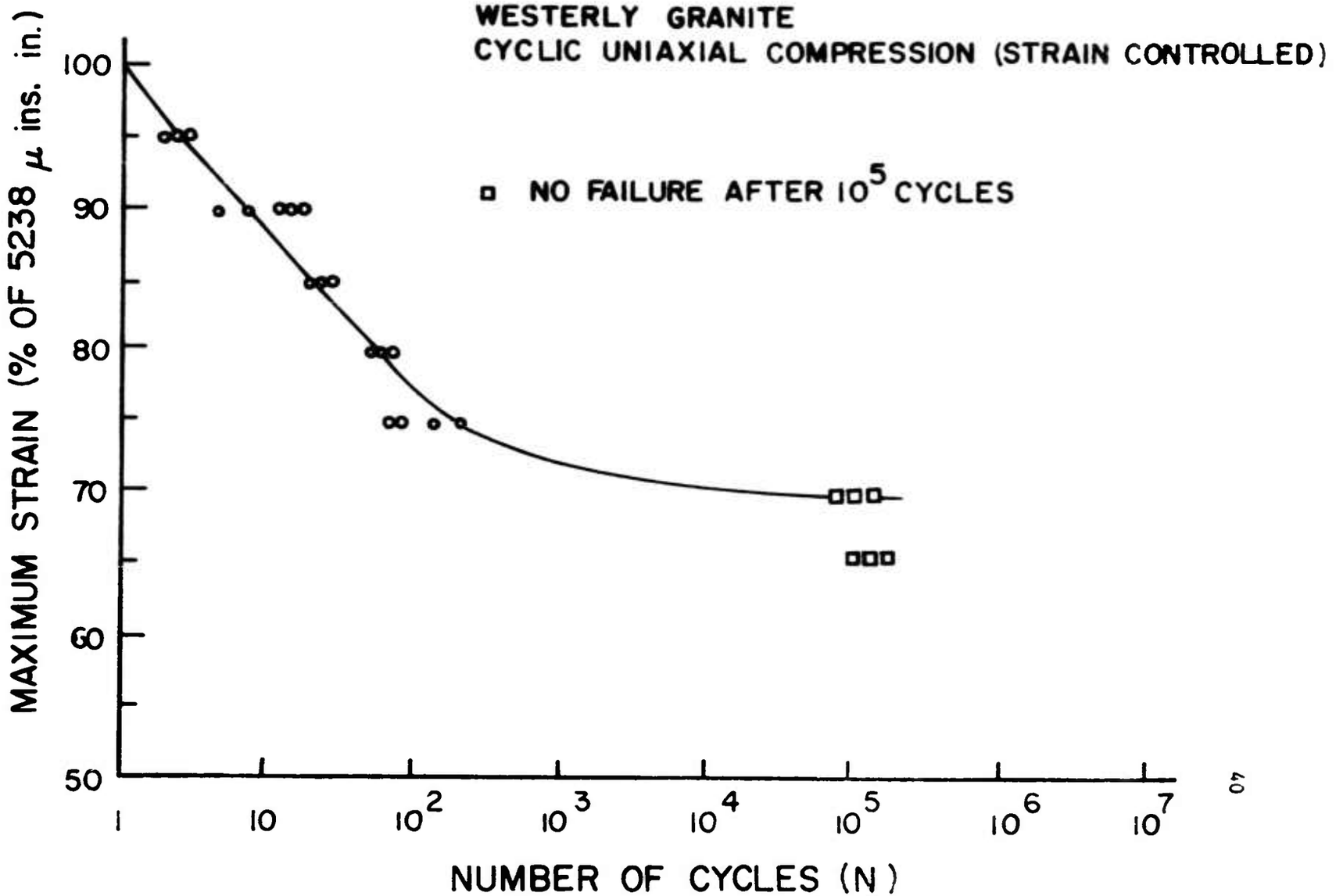

Fig. 22 E-N characteristics in uniaxial compression--Westerly granite.

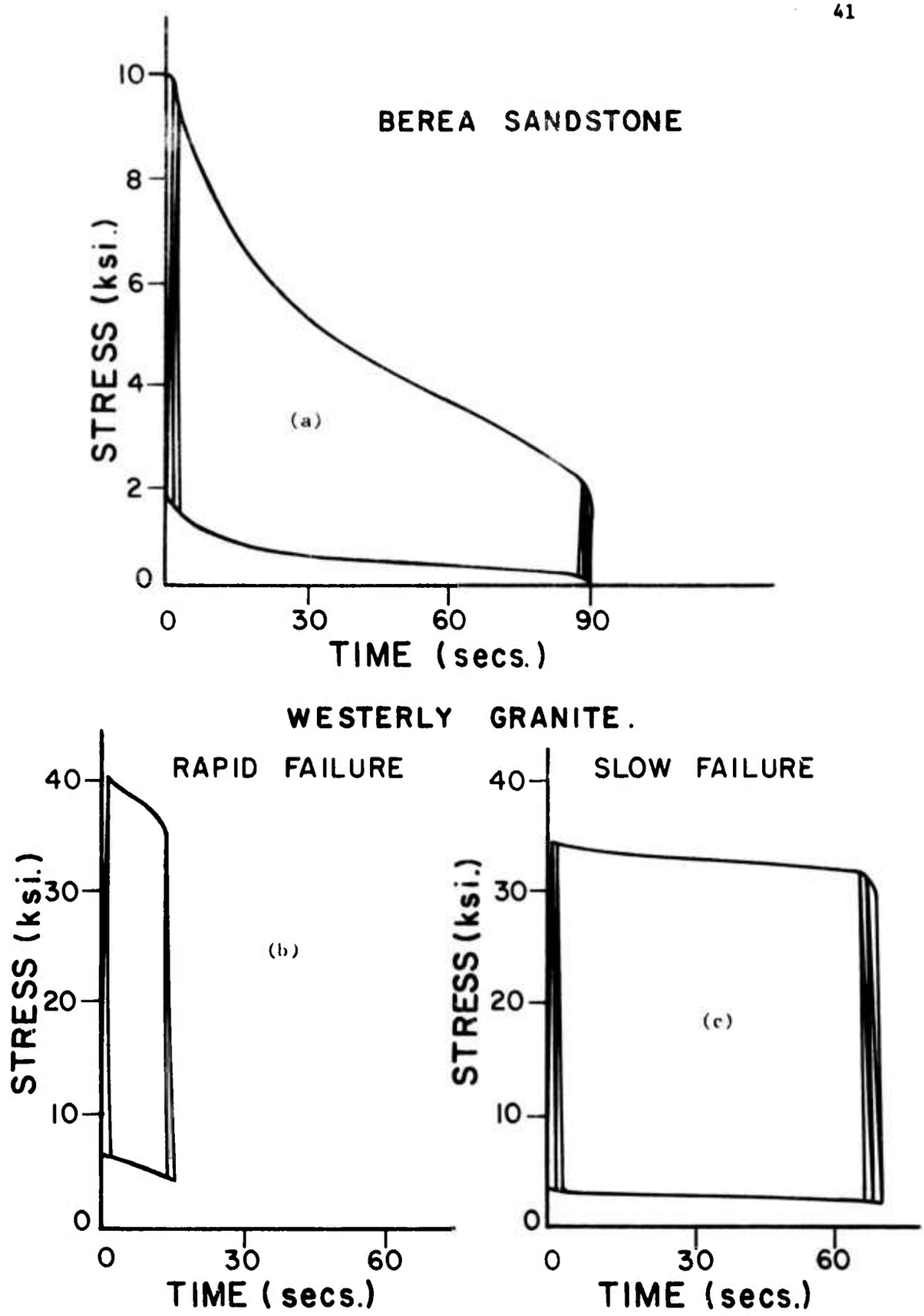

Fig. 23 Typical cyclic stress relaxation curves.

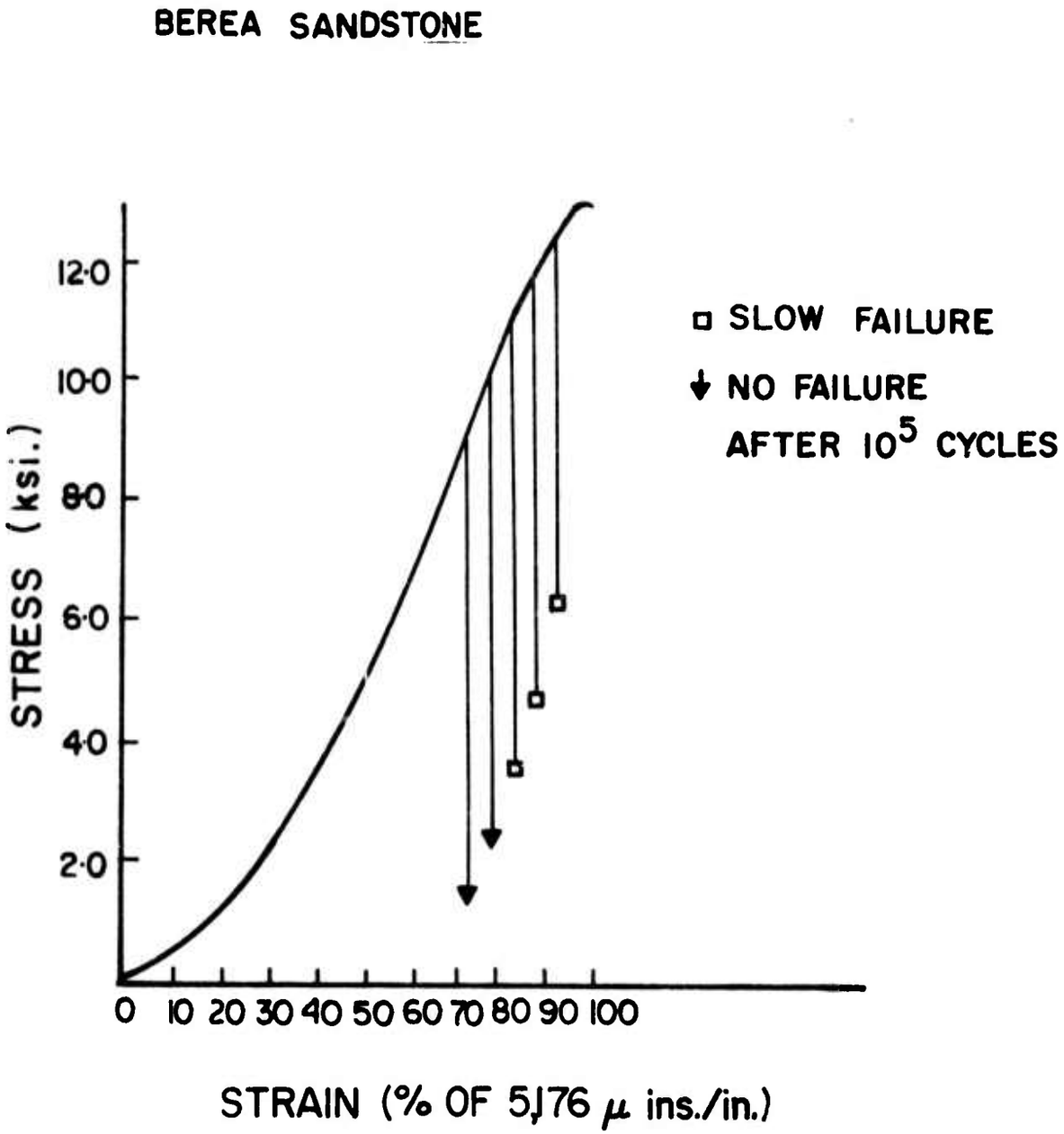

Fig. 24 Upper peak stress drop at different cyclic peak strain levels-Berea sandstone.

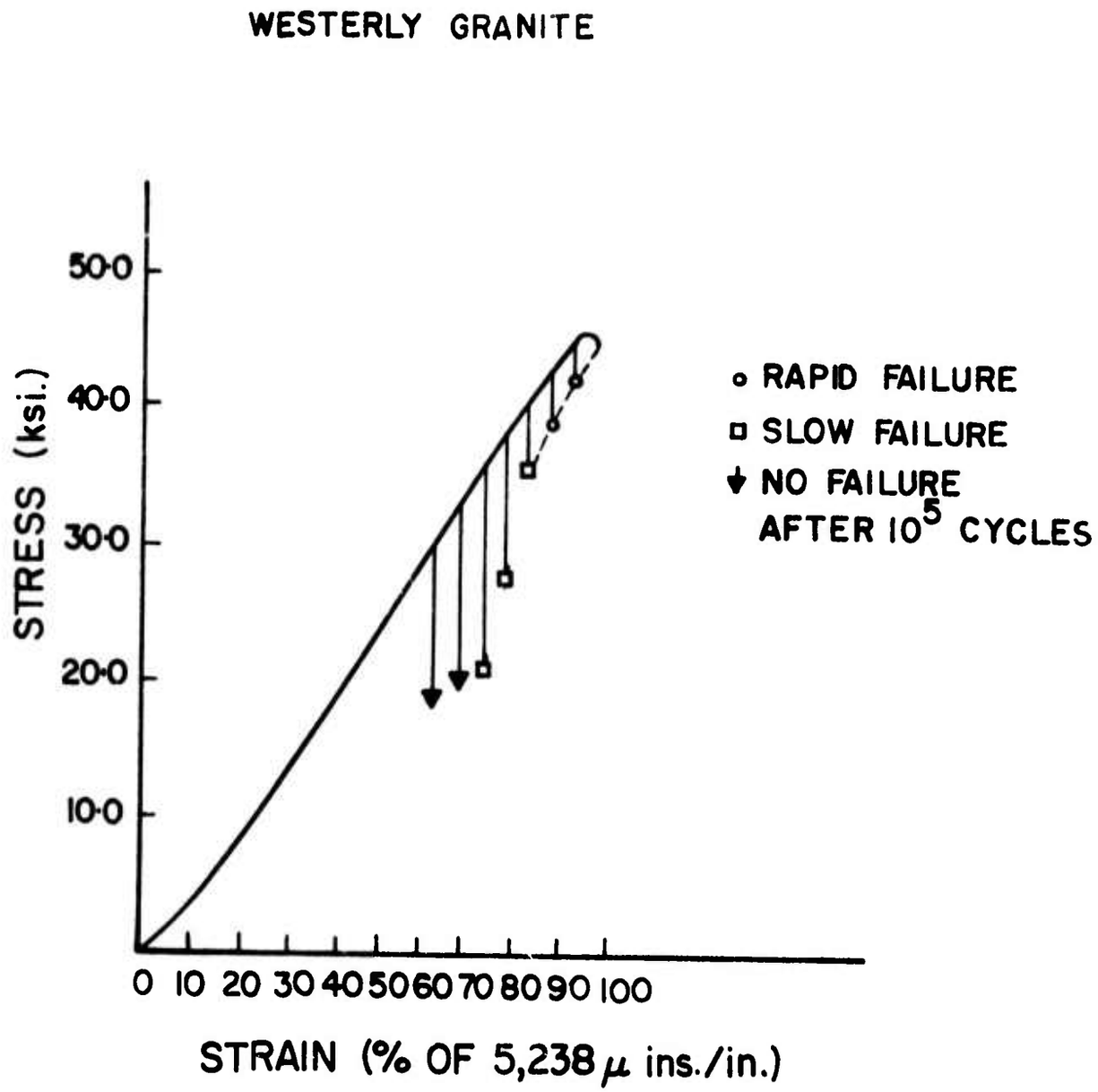

Fig. 25 Upper peak stress drop at different cyclic peak strain levels-Westerly granite.

average recorded cyclic relaxation of upper peak loads versus a complete stress-strain curve for Westerly granite. The function of the stress-strain curve as an envelope of admissible cyclic creep and relaxation is easily noted. Knowledge of the complete stress-strain curve for a particular rock could be used to predict amount of cyclic deformation or relaxation to failure, without actually running lengthy cyclic tests.

Microscopic Examination

A microscopic investigation was carried out in Westerly granite specimens that had been subjected to compressive cyclic loading between 200 psi and 35,000 psi (75% of compressive strength). Specimens were removed at different stages of their fatigue life, vertically sectioned and polished surfaces and thin sections prepared and studied under a Zeiss Ultraphot II microscope. The amount of microcracking in granite appears to be considerably less detectable than in Tennessee marble (1). Figures 26 and 27 are typical photomicrographs of thin sections of cyclically loaded granite specimens. The specimen shown in Fig. 27 was removed after 15 cycles (secondary stage). It shows an increased number of faint intergranular randomly oriented cracks within the quartz crystals. Specimens removed at different other stages of fatigue life showed very similar features. Right before failure intragranular cracks are also observed, and a widening of the felspar twin lamellae is apparent.

Figure 26 is a photomicrograph of a granite specimen that had been cyclically loaded in strain control to 75% of its maximum strain. The specimen was removed when chipping became noticeable but before total failure. The long, wide, intragranular, vertical cracks are very clear and depict an advanced stage of fatigue which only because of the type of loading has not resulted in explosive failure. The lack of such convincing cracks in the stress controlled specimens could be attributed to the fact that when final coalescence occurs crack instability results and the specimen fails before it becomes possible to remove it for further studies. Thus a specimen removed in the tertiary stage, has probably not reached the very critical stage of microfracturing prior to fatigue failure. It is apparent, however, that the internal mechanism of fatigue is one of microcracking, just like in the rocks previously examined (1).

Fig. 26 Photomicrograph of a specimen after 60 cycles of loading (upper peak strain = 75% in strain control (25X).

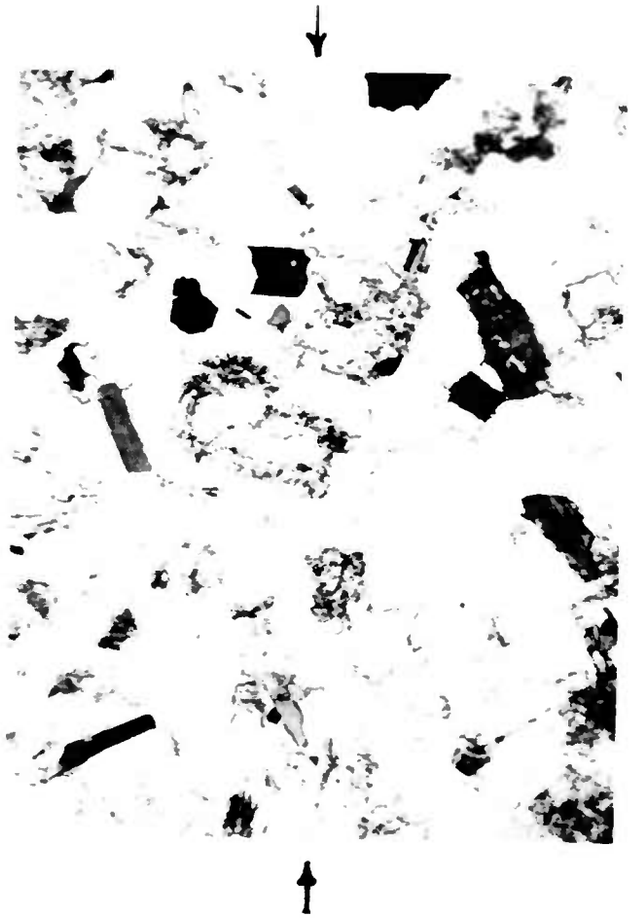

Fig. 27 Photomicrograph of a specimen after 15 cycles of loading (upper peak stress = 75%) in stress control (25X).

B - TRIAXIAL COMPRESSION

For the purpose of achieving a closer simulation of real stress conditions underground, a triaxial cell was utilized for the application of confining pressure to cyclically loaded Westerly granite specimens. The confining pressure was kept approximately constant during the tests while the vertical load was cycled as in the uniaxial case. The fatigue resistance under triaxial conditions was expected to be stronger than that of uniaxially tested samples (5).

Confining pressures of 1,000 psi and 2,500 psi were applied and appropriate S-N curves obtained. As expected both the quasi-static and the dynamic (equivalent to 1 cps) compressive strengths of the granite increased considerably with confining pressure (Table 3). The S-N curves are strikingly similar in shape to that recorded under uniaxial conditions. But as Fig. 28 shows the fatigue strength at each level of cycling is drastically increased. The speculation offered earlier regarding the shape of the S-N curve for uniaxial compression could be repeated for the case of triaxial conditions, in as much as the shape of the complete stress-strain curves remain basically the same (see Fig. 7).

Specimen deformation was measured by two DCDT transducers mounted on the outside of the triaxial cell. The Young's modulus values recorded during the first cycle showed a slight increase with confining pressure (Table 3). The stress-strain curves were similar to those recorded under uniaxial compression leaving a large amount of permanent strain in the first cycle, and being characterized by cyclic creep similar to that observed in static fatigue.

The acoustic emission from triaxially loaded specimens was detected by a piezoelectric transducer bonded to the outside of the cell. The microseismic activity appeared similar to that of unconfined specimens. The sudden acceleration in the number of events prior to failure could be used as a warning signal in actual situations. The type of failure in triaxial cyclic tests was invariably by faulting along a plane roughly at 30° to the vertical. Cyclic loading of triaxially failed specimens could not be undertaken because the DCDT transducers were not amenable to strain controlling through the MTS machine.

TABLE 3

COMPRESSIVE STRENGTHS AND TANGENT MODULI AT DIFFERENT CONFINING PRESSURES IN WESTERLY GRANITE

Confining Pressure (psi)	No. of Specimens Tested	Static Comp. Strength (psi)	Dynamic Comp. Strength (1 cps) (psi)	Tangent Modulus ($\times 10^6$ psi)
0	7	38, 200	46, 500	10. 4
1000	6	50, 400	59, 800	11. 2
2500	6	62, 500	70, 400	12. 1

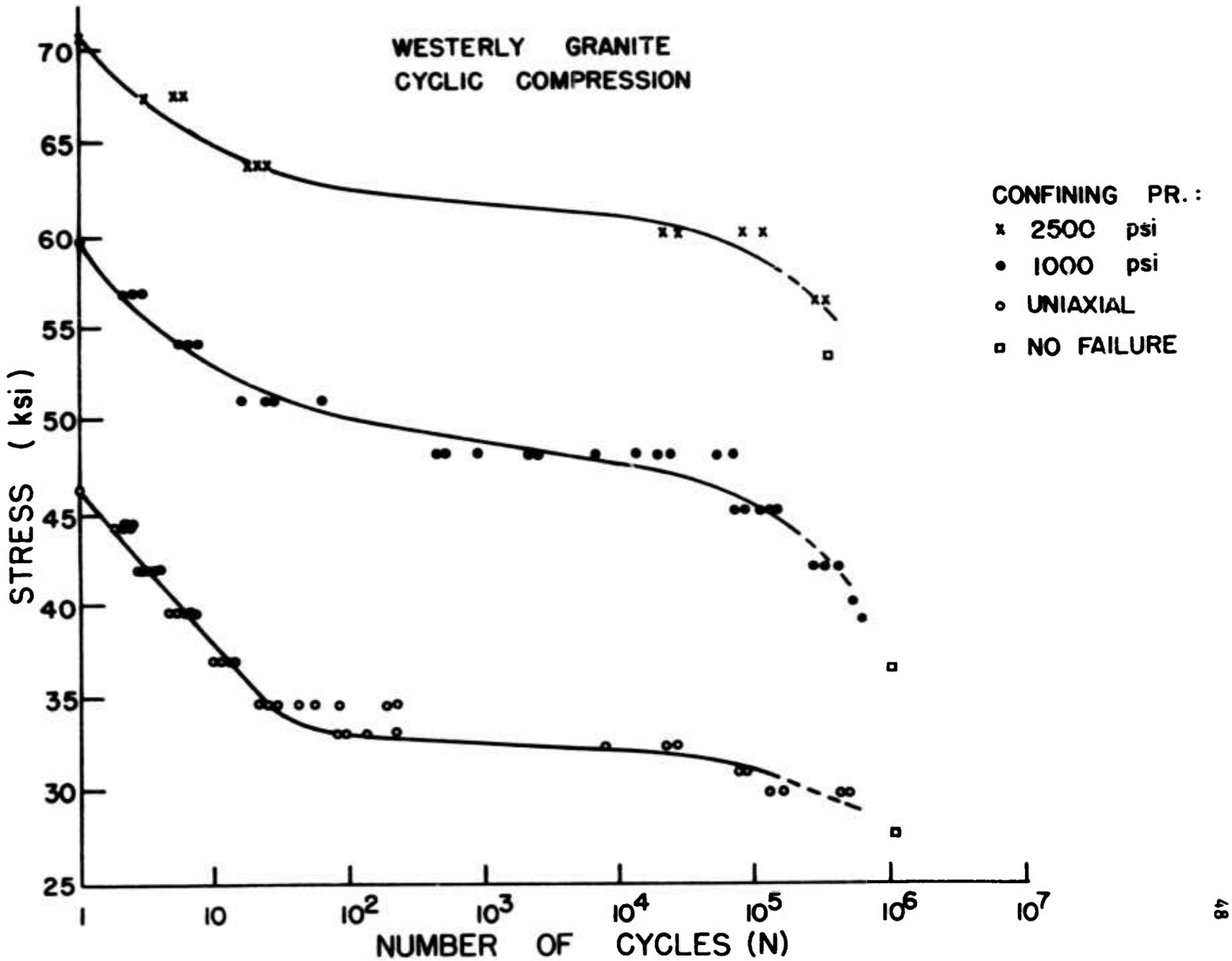

Fig. 28 S-N characteristics at different confining pressures--Westerly granite.

In general, this series of tests was in agreement with the ones run in Berea sandstone by Burdine (5). As confining pressure is raised the danger of rock failing in fatigue for the same level of stress is categorically reduced. It remains to be seen, however, what is the effect of cycling both the horizontal and the vertical stresses. The latter cyclic mode is actually a more realistic simulation of earthquake loading.

C - UNIAXIAL TENSION

All cyclic tension tests were run in stress-control, at 1 cps. for a maximum of 10^5 cycles. In the previous annual report (1) partial results were presented, based on the experimental work performed in White and Pink Tennessee marble. In this report further results in marble and new work in Indiana limestone, Westerly granite and Berea sandstone are described. Berea sandstone tests were all run in specimens with bedding planes parallel to their axis.

S-N Characteristics

The S-N characteristics were determined by keeping the lower peak stress constant (about 20 psi for Berea sandstone and 50 psi for other rocks) throughout the testing program and varying the upper peak stress from test to test. As expected in tension tests of brittle materials, scatter was rather severe. It did not obscure, however, the general trend of rock mechanical reaction to cyclic loading.

In addition to the completion and correction of an already reported curve (1) (Fig. 29), three additional S-N curves were obtained (Figs. 30, 31 and 32). Within the range of maximum cycles per test used (10^5 cycles) straight line approximations appear to best fit the experimental S-N points. The equations for the best fit linear S-N curves are given in Table 4. The apparent dynamic tensile strengths of the four rocks, at a loading rate equivalent to 1 cps., as determined from the intercept of the S axis with the S-N curve, the fatigue strengths at 10^5 cycles and the static strengths are given in Table 5. Due to the scatter involved, it appears that as a practical application of these results, a value equal to 50% of the static tensile strength could safely be used as a more realistic strength value in the design of hard rock structures subjected to uniaxial tension (static, dynamic or cyclic).

The Effect of Lower Peak Stress

A number of tests were run in Indiana limestone and Westerly granite to determine the effect of cyclic stress range on fatigue behavior. In both rocks the upper peak load was kept constant during these tests (Fig. 33), while varying the lower peak from test to test. The cyclic frequency

TABLE 4

LINEAR S-N CURVE REPRESENTATION FOR UNIAXIAL CYCLIC TENSION

Rock Type	Tensile Strength (Equivalent to 100%) (psi)	Equation (in %)
Pink Tennessee Marble	1625	S = 100.0 - 7.0 log N
Indiana Limestone	650	S = 100.0 - 6.8 log N
Berea Sandstone	380	S = 100.0 - 7.7 log N
Westerly Granite	1600	S = 100.0 - 6.9 log N

NOTE: S = fatigue strength as a percentage of the tensile strength

N = Number of cycles

TABLE 5

TENSILE STRENGTHS AND FATIGUE STRENGTHS

Rock	Tensile Strength at 1 cps (psi)	"Static" Tensile Strength (psi)	Fatigue Strength at 10^5 cycles (psi)	$\frac{\text{Fatigue Strength}}{\text{Static Tensile Strength at } 10^5 \text{ cycles}} \times \%$
Pink Tennessee Marble	1625	1400	1100	78
Indiana Limestone	650	670	425	63
Westerly Granite	1600	1385	1050	76
Berea Sandstone (parallel to bedding)	380	330	235	71.5

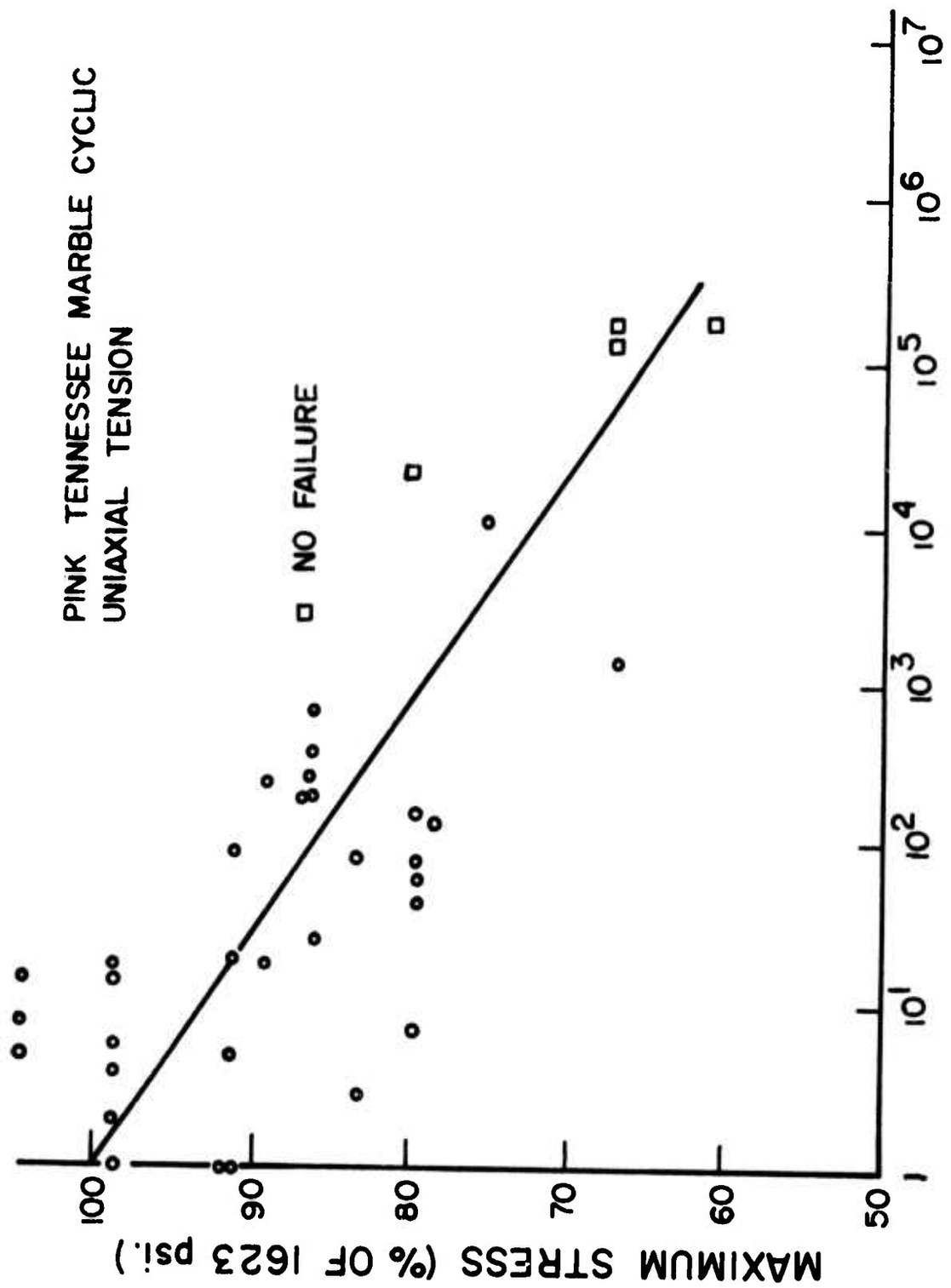

Fig. 29 S-N characteristics in uniaxial tension--Pink Tennessee marble.

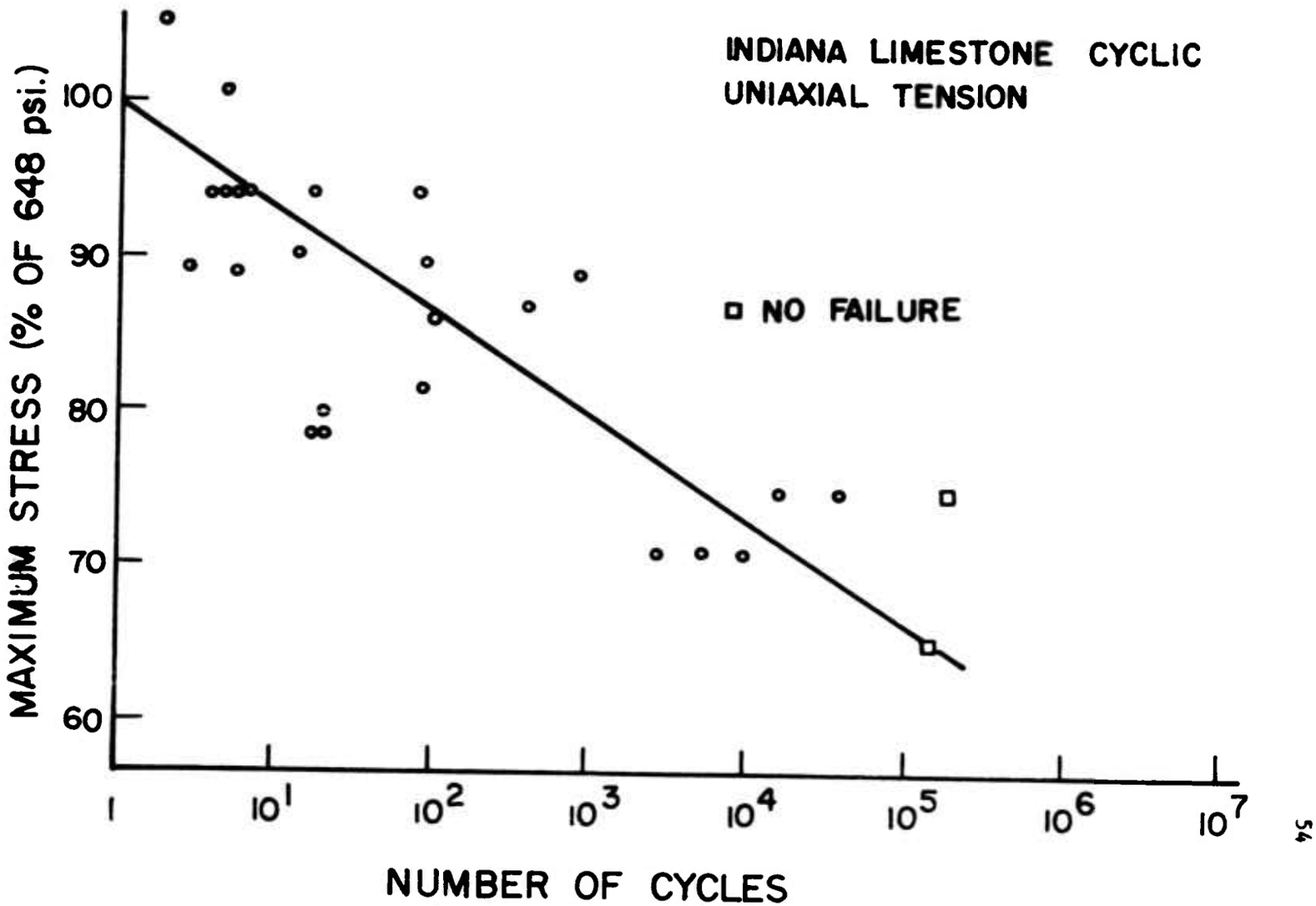

Fig. 30 S-N characteristics in uniaxial tension--Indiana limestone.

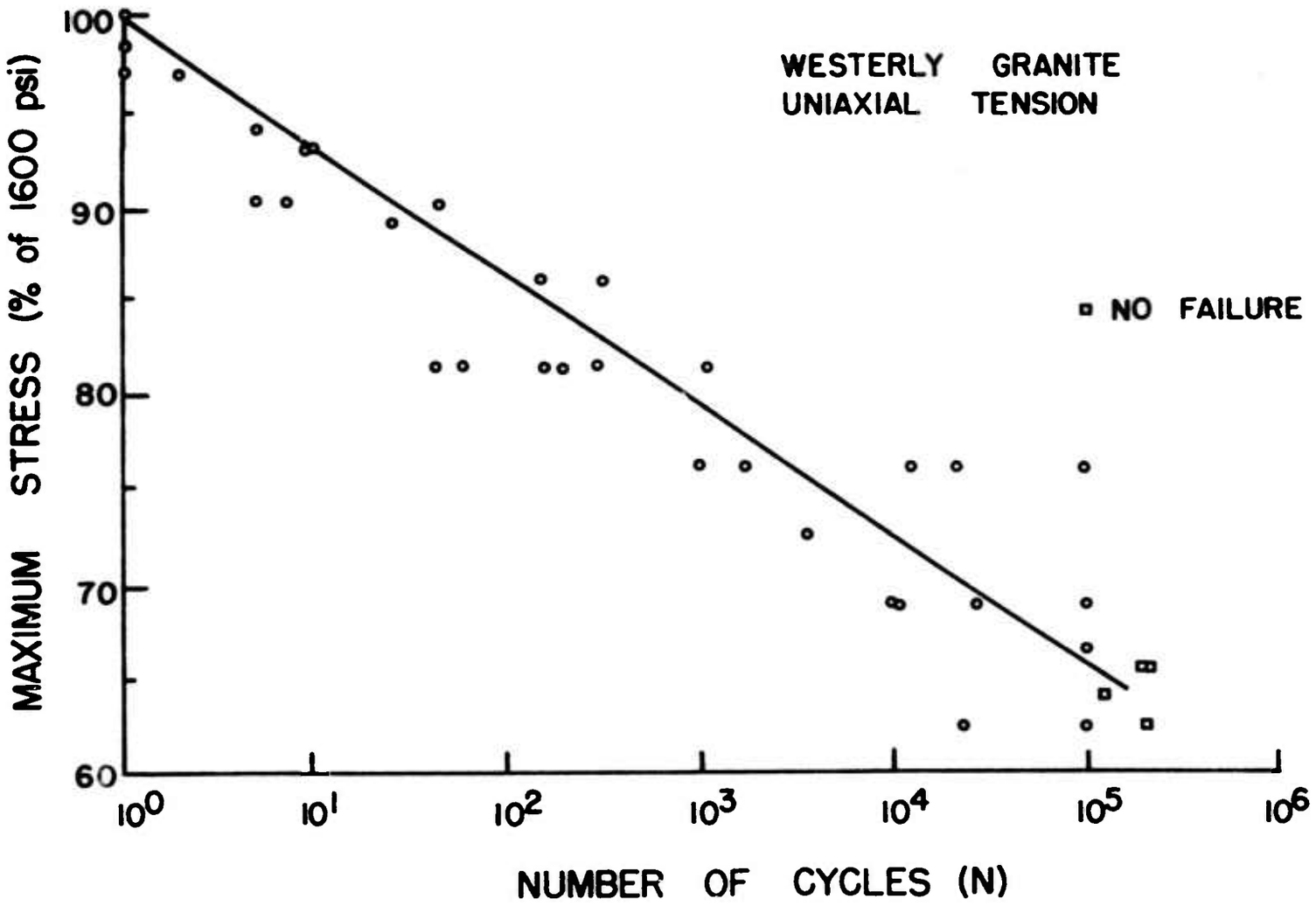

Fig. 31 S-N characteristics in uniaxial tension--Westerly granite.

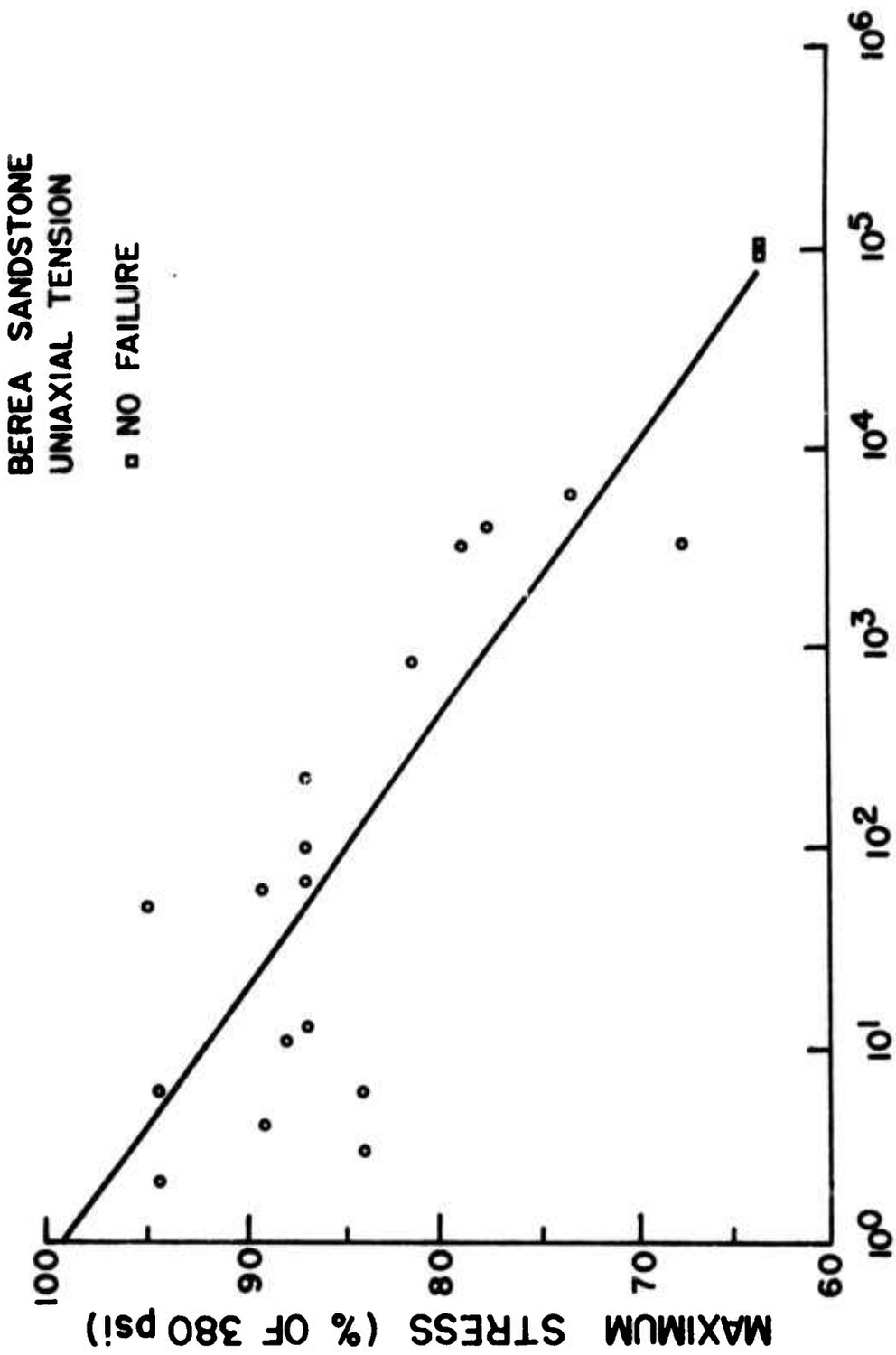

Fig. 32 S-N characteristics in uniaxial tension--Berea sandstone.

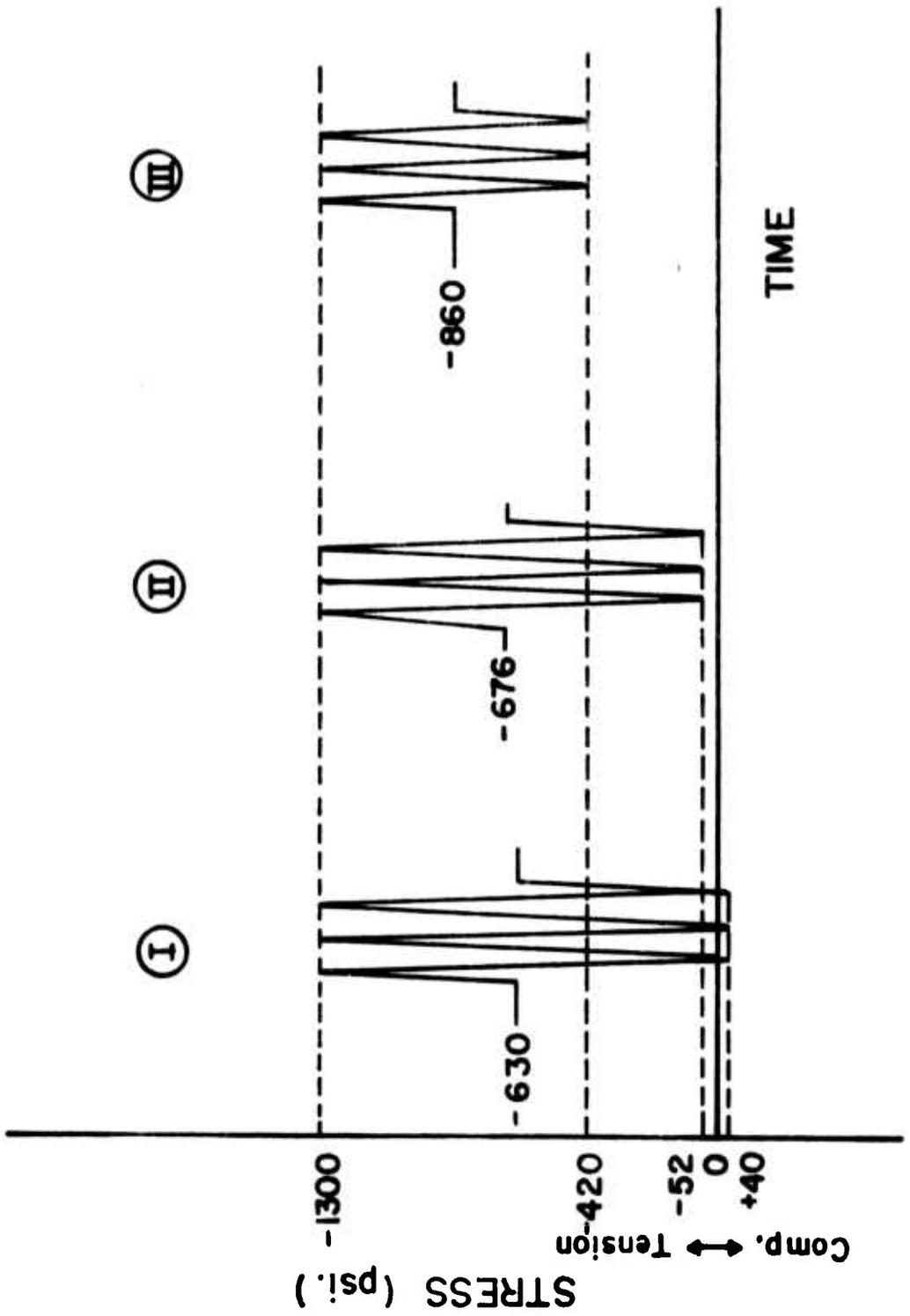

Fig. 33 Three stress amplitudes used in cyclic loading of Westerly granite.

was kept at 1 cps. In one series of tests the stress range was zero, i.e., the static fatigue strength was determined. In another series of tests the lower peak was extended into the compression zone. The results are given in Table 6 and Fig. 34.

It is apparent from these results that as the stress amplitude increases, for the same upper peak, the fatigue endurance capacity decreases. In particular, note a difference of two orders of magnitude between the static and the cyclic fatigue life in the limestone, and the considerable weakening undergone by the granite when it is subjected to a tension-compression cyclic fatigue. The large discrepancy between the static and dynamic fatigue results indicates that the mechanism of cyclic fatigue is possibly different from that of creep. The sudden decrease in fatigue life when the lower peak stress was taken into the compression zone indicated that tension-compression cyclic stresses could be most damaging and further work in that zone was undertaken.

Stress-Strain Behavior

Stress-strain behavior in cyclic tension is analogous to that in compression as described in the previous report (1). A distinguishing factor is the considerable permanent strain accumulated in tension during the first cycle of loading-unloading. Figures 35, 36, 37, and 38 show that in four different rocks the permanent strain at the lower peak stress level after one cycle is approximately equal to the cyclic creep accumulation during the remainder of the cycles to failure. This permanent strain after the first cycle in tension is considerably higher than the corresponding value in compression when compared to the total amount of unrecoverable strain. One practical application of this phenomenon is that the total cyclic creep during cyclic loading in tension could be estimated from the permanent strain recorded during the first cycle by multiplying the latter value by two (Table 7).

In three of the four rocks tested (Tennessee marble was an exception) the stress-strain loading curve of the first cycle was highly nonlinear which showed the rocks to be stiffest at very low stresses, with ever increasing softness as the upper peak stress was reached. The curve linearized considerably in the second cycle, and from then on continued

TABLE 6

EFFECT OF LOWER PEAK STRESS ON FATIGUE IN UNIAXIAL TENSION

No. of Specimens	Upper Peak Load (psi)	Lower Peak Load (psi)	Stress Range (psi)	Fatigue Life (cycles)
		Indiana Limestone		
From S-N Curve	- 600	- 50	550	14
5	- 600	-400	200	28
5	- 600	-600	0	1104 (secs)
		Westerly Granite		
7	-1300	+ 40 (compression)	1340	23
4	-1300	- 50	1250	380
5	-1300	-420	880	274

TABLE 7

TYPICAL PERMANENT STRAINS IN UNIAXIAL CYCLIC TENSION

Rock Type	Level of Loading in % of Strength	Number of Cycles at Failure	First Cycle Permanent Strain at Lower Peak μ in/in	Total Cyclic Creep at Upper Peak μ in/in	Total Permanent Strain at Lower Peak μ in/in	Ratio of Total to First Cycle Permanent Strain
Indiana Limestone	95	5	51.0	36.0	72.0	1.4
Pink Tennessee Marble	80	4	3.5	--	7.5	2.1
Berea Sandstone	85	10	784.0	1070.0	1425.0	1.8
Westerly Granite	80	2500	70.0	107.0	144.0	2.1

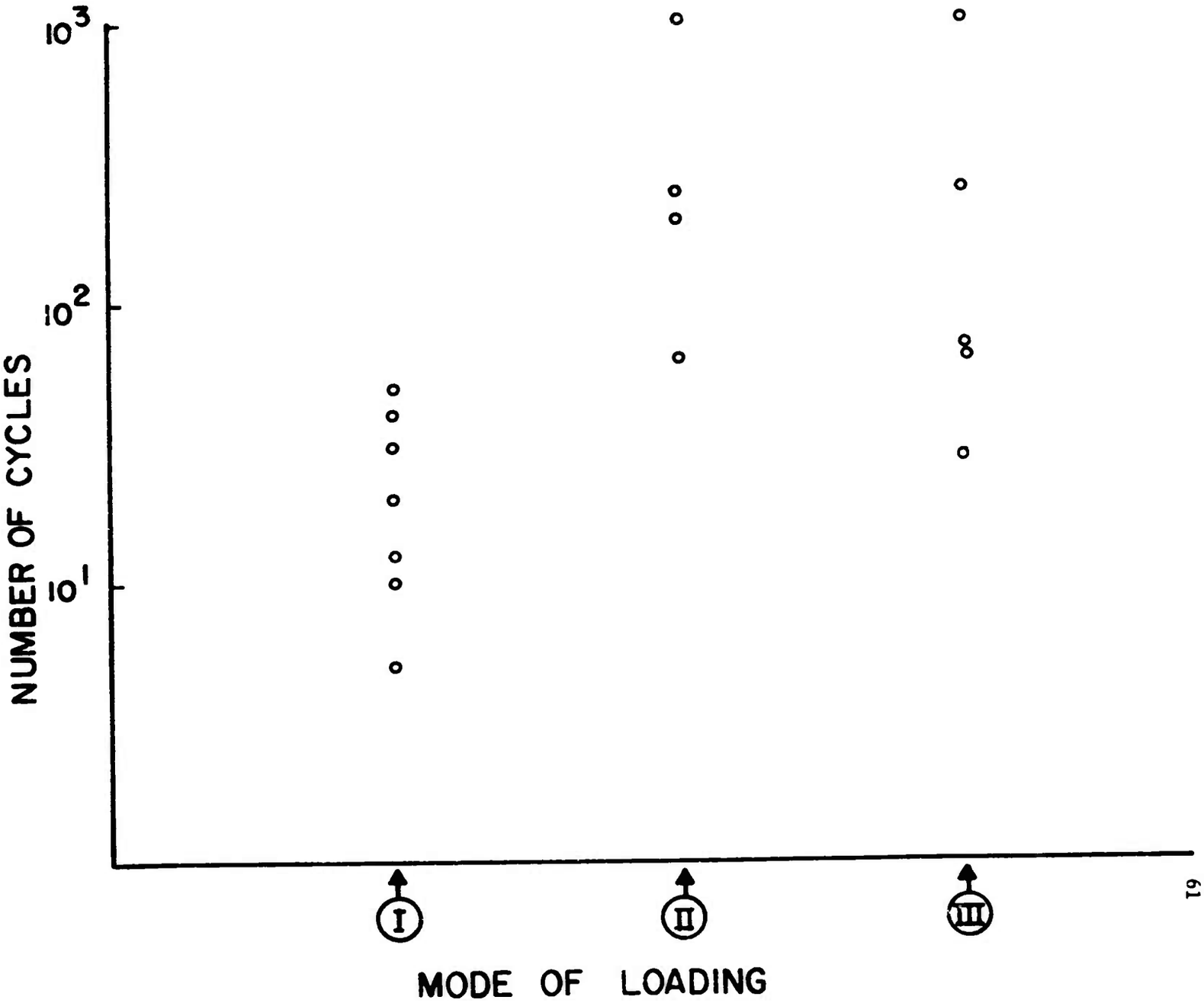

Fig. 34 Experimental results of fatigue life for three different stress amplitudes, same upper peak stress--Westerly granite.

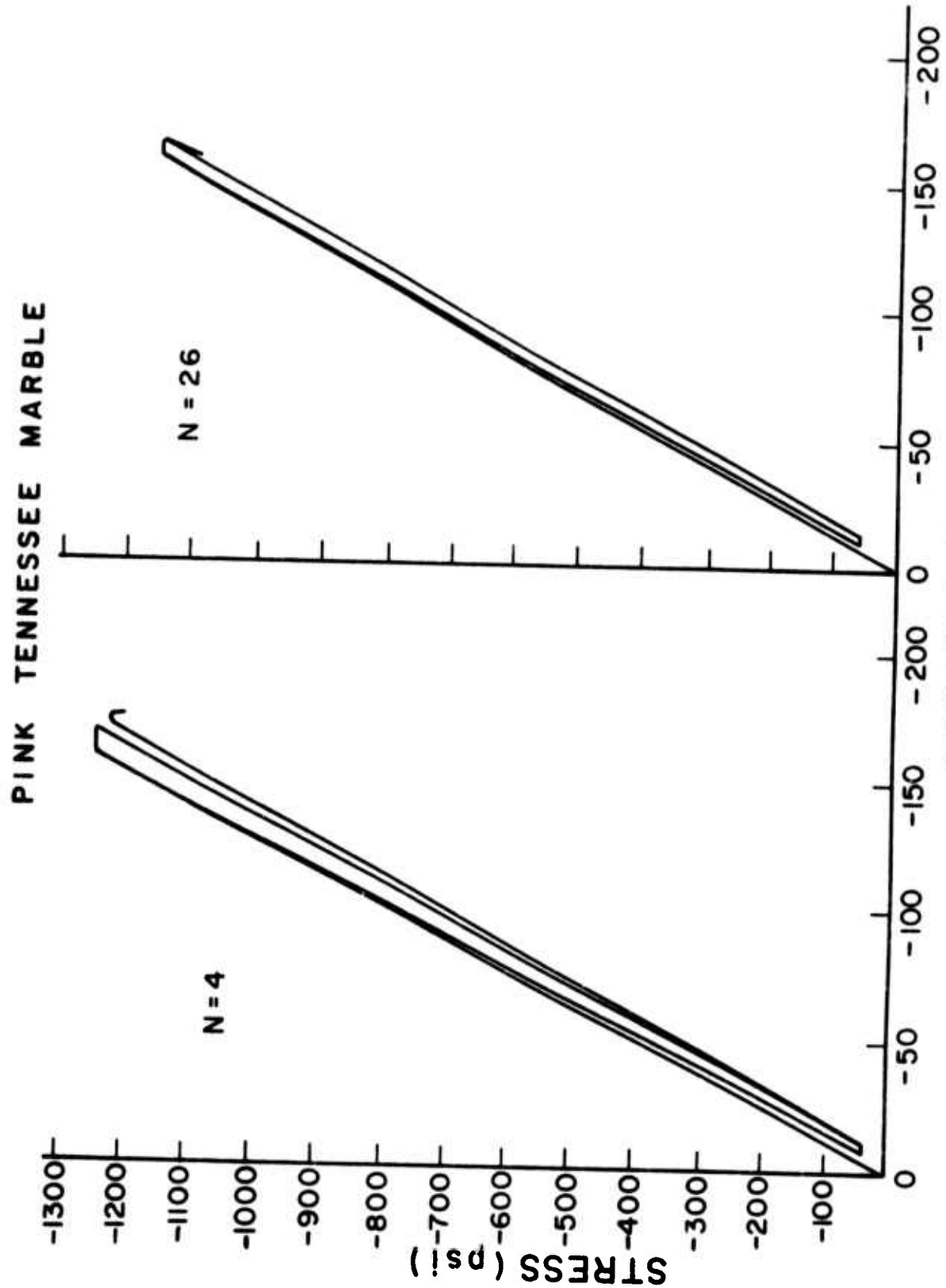

Fig. 35 Typical stress-strain curves in stress controlled cyclic uniaxial tension--Pink Tennessee marble.

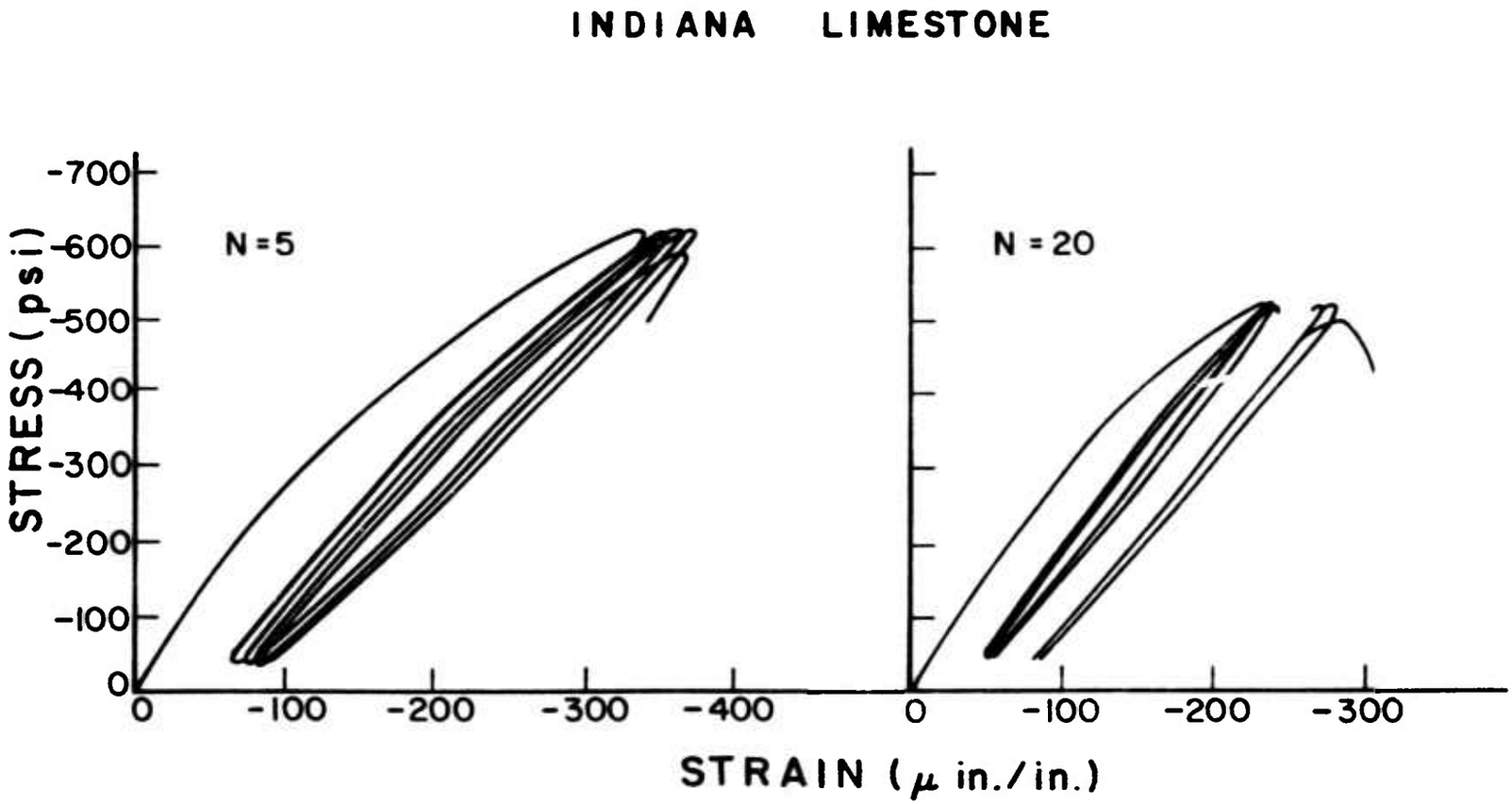

Fig. 36 Typical stress-strain curves in stress controlled cyclic uniaxial tension--Indiana limestone.

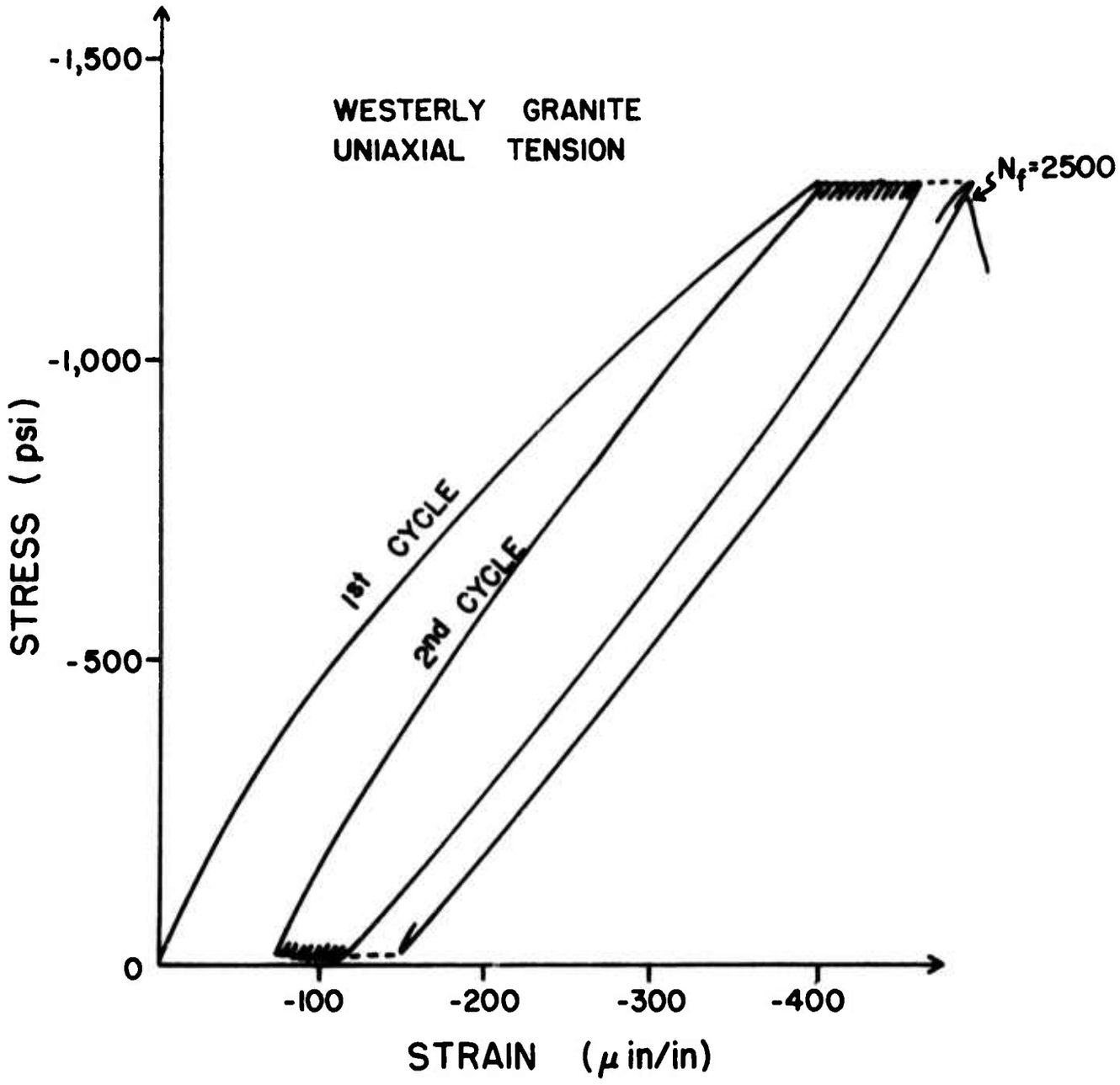

Fig. 37 Typical stress-strain curve in stress controlled cyclic uniaxial tension--Westerly granite.

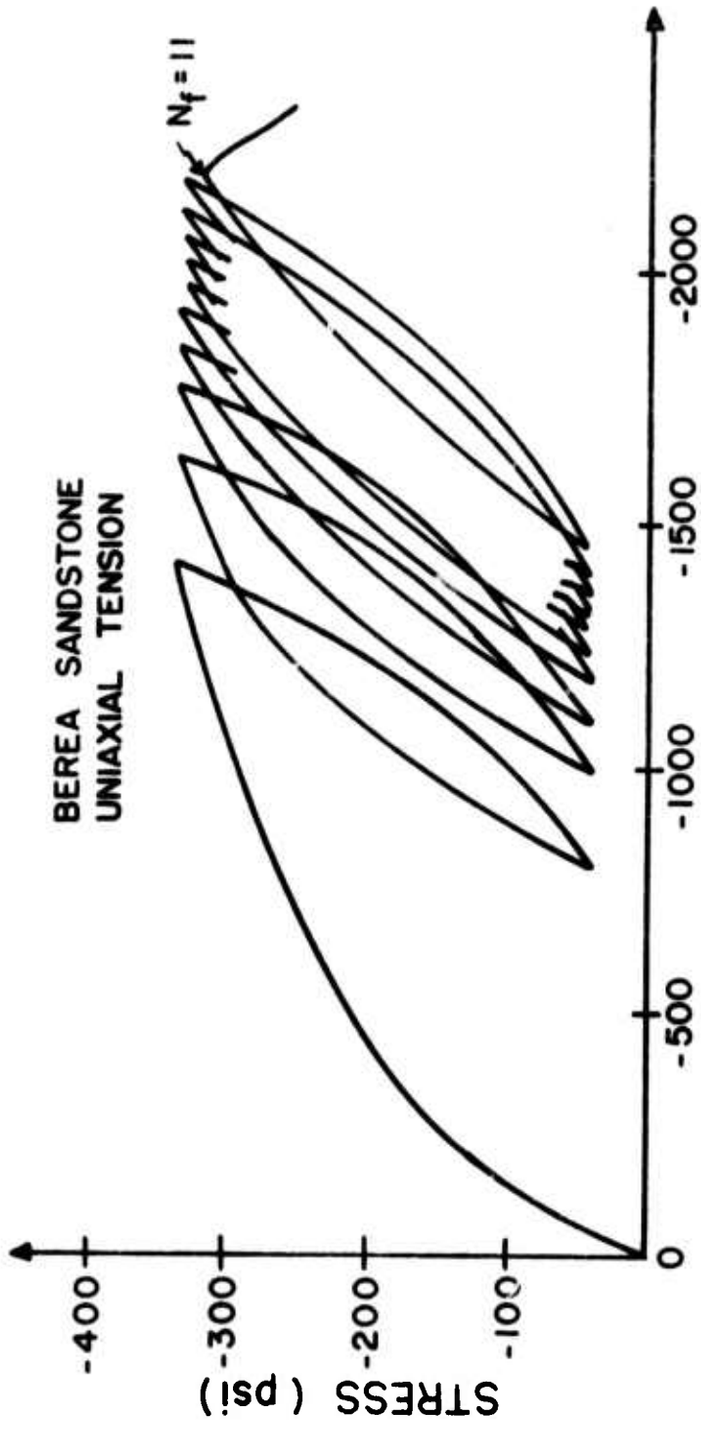

Fig. 38 Typical stress-strain curve in stress controlled cyclic uniaxial tension--Berea sandstone.

at an almost identical shape for the rest of the cycles. The average tangent Young's Modulus during the second cycle was higher than during the first cycle. The value then decreased with cycling, so that the Young's Modulus of the last cycle was not very different than that of the first cycle. (See Table 8).

From the above observation (permanent strain and stress-strain slope) it appears that the major damage to rock microstructure, i.e., opening of cracks, and/or loosening of grain boundaries, is undergone in the first cycle. Additional cycles are usually needed to extend the weakest crack to its critical length, culminating in tensile rupture. It was also noted that the third stage of the cyclic stress-strain curve, just prior to failure, was almost nonexistent in uniaxial tension in support of the assumption that tensile rupture is a localized phenomenon.

The nonlinear behavior and the amount of permanent strain accumulated in the first loading cycle could also be used to assess rock brittleness in tension for classification purposes. In the group of rocks tested the classification in order of decreasing brittleness would be: Pink Tennessee marble, Westerly granite, Indiana limestone, Berea sandstone.

Retested Specimens

As described in the previous report (1) cyclic fatigue in tension culminates in a tensile rupture not unlike that obtained in a static test. The question is whether the fatigue effect is indeed as localized as the rupture implies. In an effort to test the hypothesis of localized fatigue, a number of cyclically failed specimens were reglued together in the plane of rupture and later retested. The reconstruction of the specimens was done with the same epoxy cement used to join rock to end caps. All excess epoxy was squeezed out and utmost care was taken to ensure that the alignment of the original specimen was not disturbed by the reglueing.

The results are summarized in Table 9. Specimens initially failed after less than 10^3 cycles showed reduced fatigue resistance when retested. Those initially surviving 10^4 cycles or more showed improved fatigue

TABLE 8

TYPICAL YOUNG'S MODULUS VARIATION WITH CYCLING IN UNIAXIAL TENSION

Rock Type	Level of Loading (psi)	No. of Cycles to Failure	Tangent Young's Modulus at 50% of Peak Stress		
			1st Cycle (psi)	2nd Cycle (psi)	Last Cycle (psi)
Indiana Limestone	- 625	5	1.80×10^6	2.10×10^6	2.0×10^6
Pink Tennessee Marble	- 1240	4	7.8×10^6	8.0×10^6	7.7×10^6
Berea Sandstone	- 330	10	0.32×10^6	0.47×10^6	0.41×10^6
Westerly Granite	- 1300	2500	3.3×10^6	3.9×10^6	--

TABLE 9

INDIANA LIMESTONE RETESTED SPECIMENS

Specimen Number	Upper Peak Stress (% of tensile strength)	Fatigue Life Initial Test	Fatigue Life Retest	Monotonic Strength if Unfailed After Stated Cycles in Retest (% of Tensile Strength)
20	94	5	1	--
21	94	4	1	--
40	89	90	40	--
35	88	845	10	--
47	74	35, 700	228, 000+	91. 4
29	71	9, 260	198, 410+	101. 0

resistance. In the two very short tests, the second failure surface was 1/16 inch away from the first, suggesting that there was some secondary damage adjacent to the original failure plane. Such secondary damage in the form of a few minor additional cracks near the main one was commonly observed in both monotonic and fatigue failed specimens. In the other specimens the second failure surface was at least 1/4 inch from the original and usually farther away. This seems to suggest that less secondary failure occurred in these specimens. If the specimens had been completely homogeneous and if fatigue damage had been uniformly distributed over the specimens, all of them would have failed during the first cycles of the retest. That they did not, and that some were actually stronger the second time suggests two hypotheses: (a) tensile fatigue failure in rock is quite localized, (b) fatigue damage becomes increasingly localized at smaller stresses.

Microscopic Examination

A microscopic investigation was undertaken in Indiana limestone and Tennessee marble. Most of the microscopic work was conducted on polished vertical sections of untested and tested (failed) specimens. In addition, in some Pink Tennessee marble specimens portions of the outside surface was polished prior to testing, photographed, subsequently fatigued and re-examined for before and after differences.

Most microscopic examination and all photomicrography utilized the Zeiss Ultraphot II camera microscope. This instrument provides a vertical light source. For oblique light a Bausch and Lomb microscope light was used.

Indiana limestone is porous with pores of a wide variety of shapes and sizes (Fig. 39), and some hairline cracks are visible under oblique illumination. Pink Tennessee marble has no visible porosity. (See Fig. 40). The only significant defects are numerous hairline cracks. They are fairly randomly oriented and range in length to at least 1/4 inch. They are particularly numerous in coarsely crystalline areas of the rock but are not limited to any crystal size and many extend far beyond single crystals. Most of these cracks are only visible in oblique light, meaning that crack width is very small. Most are probably partially resealed and

Fig. 39 Photomicrograph of a virgin Indiana limestone specimen (40X, oblique illumination).

Fig. 40 Photomicrograph of a virgin specimen of Pink Tennessee marble specimen (40X, vertical illumination). The sets of parallel lines are twinning striations.

may exhibit substantial cohesion. Twinning was abundant with up to about 5,000 twinning striations/inch in some crystals. (See Fig. 40). Many crystals showed more than one twinning direction, sometimes with visible offsets in the older twin bands.

No microstructural change due to fatigue could be detected in Indiana limestone. However, no specimens were photographed before and after testing, so subtle changes such as a small increase in the number or length of cracks or the occurrence of additional twinning could have gone undetected. It seems quite likely that one or both of these phenomena took place.

Pink Tennessee marble specimens were not appreciably changed by fatigue. Tested prephotographed specimens could not easily be distinguished from untested ones. One specimen had one recognizeable new crack, see Fig. 41 and 42, at 85° to the direction of loading. It was 1/32 inches long and 3/4 inches from the final failure surface. Another specimen had a new crack at 45° to the loading direction. It was 1/16 inch long and 1/4 inch from the final failure surface. Both cracks are very close to other cracks and both may have started along those other cracks, or they may have stopped at them. No new cracks could be found in a third specimen. While a few new cracks were probably missed, particularly very small ones, it is significant that the number of cracks increased by substantially less than 1%. No pre-existing cracks were found to have extended in any of the specimens.

It was found in the pre-photographed specimens that the final failure surfaces followed pre-existing cracks for most of their lengths. It would appear that these features are the critical flaws in Pink Tennessee marble. Fatigued and monotonically loaded specimens were undistinguishable under the microscope.

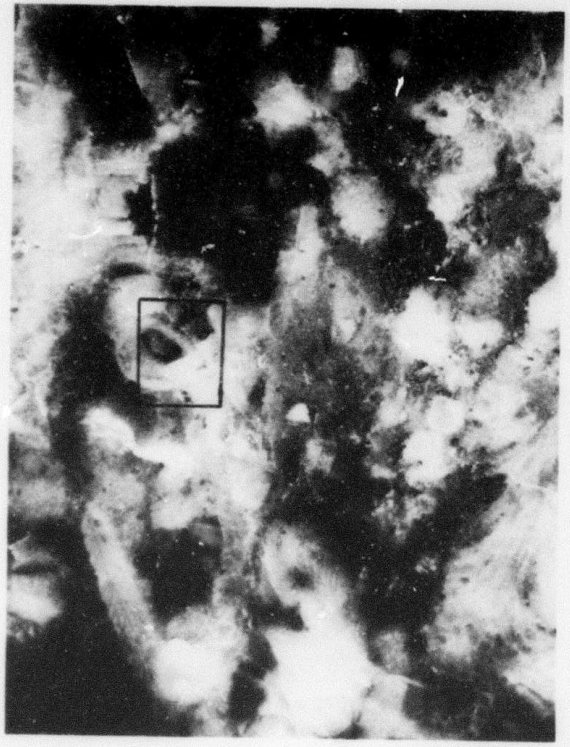

Fig. 41 Photomicrograph of a specimen of Pink Tennessee marble prior to loading (8.5X, oblique illumination).

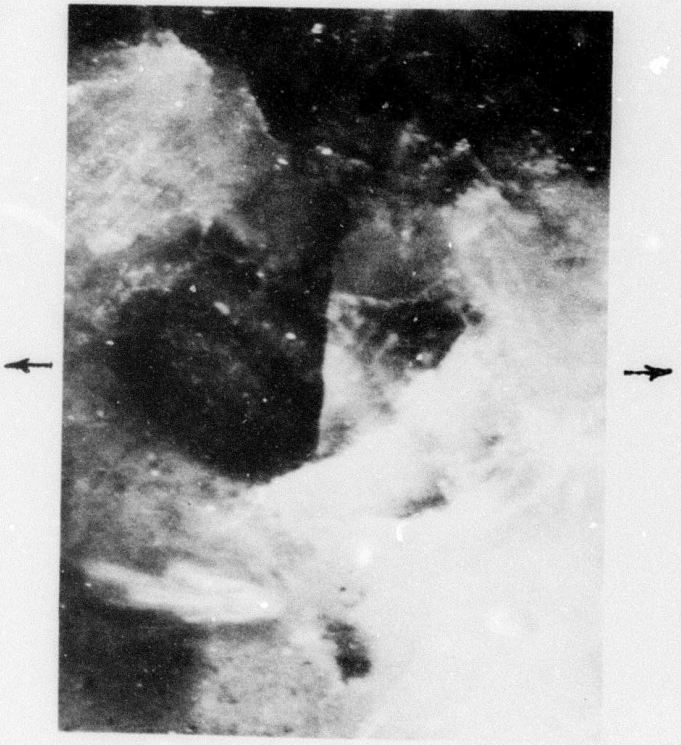

Fig. 42 Photomicrograph of a specimen of Pink Tennessee marble showing a new crack due to fatigue in direct tension (40X, oblique illumination).

D - UNIAXIAL TENSION-COMPRESSION

A series of tests was undertaken in Westerly granite subjected to cyclic uniaxial tension-compression. This type of loading can often occur during earthquakes, blasting, drilling, etc. The mechanical behavior of rock under compression only, or tension only, has been thoroughly studied and to a great extent established. But little is known about the reaction of rock to stresses that vary from tension to compression and vice versa. Therefore, before undertaking any cyclic testing, a series of quasistatic tests were run to establish basic stress-strain behavior. The experimental set-up was essentially the same as in uniaxial tension, except that the end caps were hardened and bolt size increased to facilitate for the high compressive stresses. A pair of DCDT's were used to monitor strain in the specimens (Fig. 1).

A typical stress-strain curve for Westerly granite is shown in Fig. 43. The specimen was first loaded in compression to 10,000 psi, unloaded, and loaded in tension to +1,300 psi, recompressed and then pulled to failure at 1,500 psi. One major peculiarity of the stress-strain curve is the severe "softening" of the rock in the tensile zone. The average tangential Young's modulus dropped from 8.4×10^6 psi in compression to 2.4×10^6 psi in tension. This change in material characteristics is usually ignored in calculating stresses in rock, but has been found to have substantial effects on the rock stress distribution (6). The decrease in the tensile Young's modulus could be attributed to the opening of existing cracks in pulling. The large permanent strain in unloading indicates that some of these cracks were opened beyond their elastic limit. The stress-strain curve itself forms a closed hysteresis loop whose area is proportional to the amount of energy dissipated in loading a rock specimen in tension-compression.

The cyclic tension-compression tests were run mainly with the intent of observing the effect of compressive loading on tensile cyclic fatigue. The stress range was kept constant at 10,000 psi and the tensile peak stress was varied from test to test between the dynamic tensile strength value and the fatigue strength at 10^5 cycles. The compressive peak stress was varied accordingly, so as to keep the stress range constant (18 to 20% of the dynamic compressive strength). As it may be expected all the

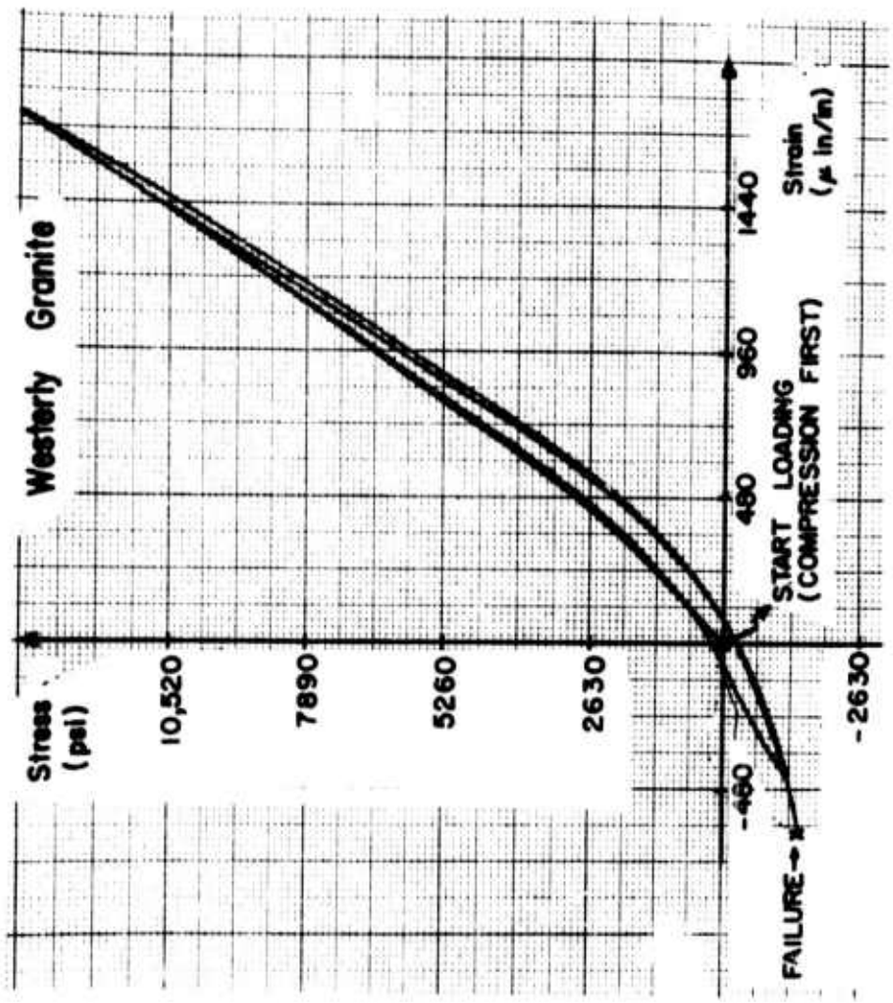

Fig. 43 Stress-strain curve in tension-compression quasistatic loading--Westerly granite.

specimenstested failed in tension along a plane normal to the direction of loading. But most significant was the fact that the fatigue strength at 10^5 dropped from 1,000 psi (60%) in pure tension to 500 psi (33%) in tension compression. At every peak level of cycling the number of cycles required to fatigue the rock was considerably reduced in tension-compression. At every peak level of cycling the number of cycles required to fatigue the rock was considerably reduced in tension-compression, and the resulting S-N curves is much steeper than in pure tension (Fig. 44). This very significant result implies that the most damaging type of cyclic loading is tension-compression. The level of 33% of tensile strength as the fatigue strength for 10^5 cycles really means that rock (or at least Westerly granite) has very little resistance to tension-compression cycling. This should serve as a warning in as far as design in rock is concerned. It is at the same time an encouraging result for rock drilling and fragmentation design. A relative comparison between the S-N curves for different types of cyclic loading in granite is shown in Fig. 45.

The stress-strain behavior is typified by Fig. 46. While the cycle portions on the compression side showed almost no changes, on the tension side the initial permanent strain after the unloading of the first cycle, and the total cyclic creep at peak tension were large and significant. In particular the tangential Young's modulus at 50% of peak tension level reduced by 30% from 3.1×10^6 psi in the first cycle to 2.1×10^6 psi in the last cycle! A definite cyclic dependent softening was obtained and its effect on the tensile strength was determined by monotonically loading to failure those specimens that survived 10^5 cycles. As shown in Table 10, 30% strength reduction was obtained in tension-compression specimens, whereas no significant changes were observed in specimens originally loaded in tension only.

No microscopic or other studies have been run so far to determine the mechanism of accelerated rock fatigue due to tension-compression. However, it is postulated that the basis for the effective cyclic weakening is the complete closing in compression of cracks originally opened in tension.

TABLE 10

TENSILE STRENGTH REDUCTION AFTER CYCLIC LOADING IN WESTERLY GRANITE

Test No.	Initial Tensile Strength (psi)	Initial Cyclic Loading			Secondary Monotonic Loading	
		Upper Peak (psi)	Lower Peak (psi)	No. of Cycles	New Tensile Strength (psi)	Strength Reduction (%)
T 72(B)	1, 600	-1, 000	-50	110, 000	1, 550	3. 1
T 74(B)	1, 600	-1, 050	-50	178, 000	1, 500	6. 3
T 75(B)	1, 600	-1, 050	-50	162, 200	1, 580	1. 0
T132(B)	1, 600	-650	+9, 350	89, 000	1, 100	30. 0
T133(B)	1, 600	-650	+9, 350	110, 700	1, 160	27. 5

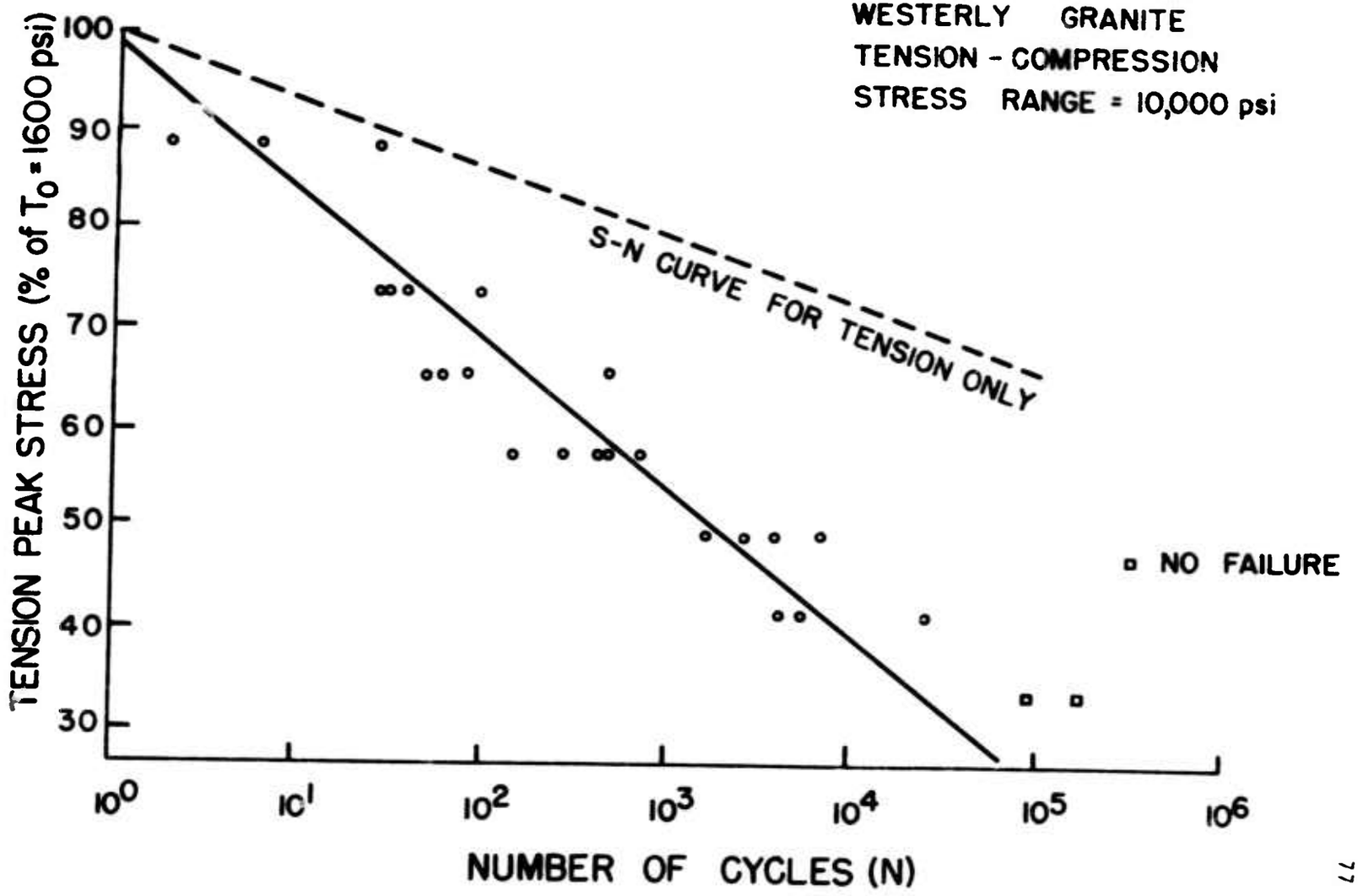

Fig. 44 S-N characteristics in uniaxial cyclic tension-compression--Westerly granite.

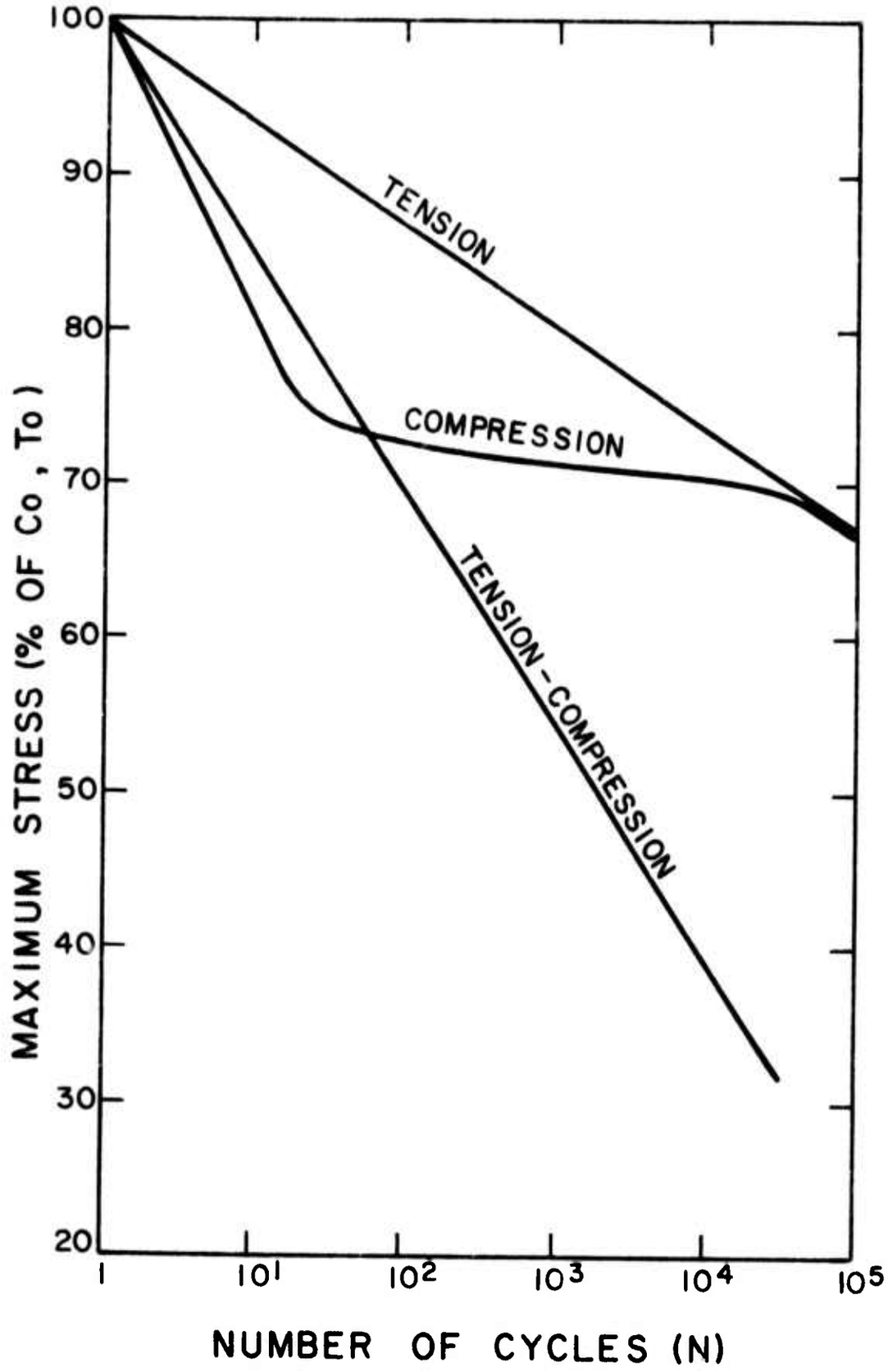

Fig. 45 S-N curves for the three loading types in Westerly granite.

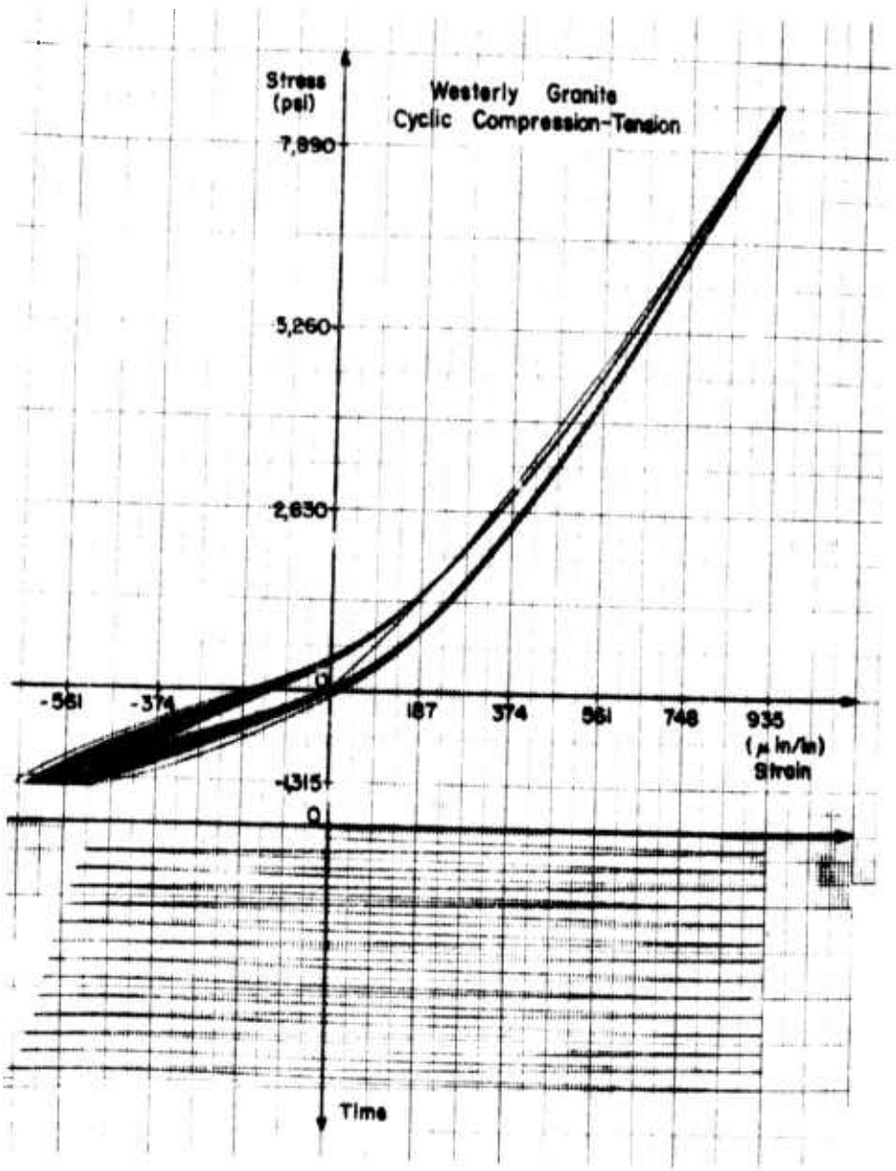

Fig. 46 Stress-strain and strain-time curves in stress controlled cyclic tension-compression--Westerly granite.

CONCLUSIONS AND PRACTICAL APPLICATIONS

The experimental work carried out for the present contract confirmed for additional hard rock types some of the conclusions presented in the first annual report, and contributed new and important findings of its own.

1. Berea sandstone and Westerly granite, like the previously tested Tennessee marble and Indiana limestone were weakened considerably by cyclic uniaxial compression. Indiana limestone, Berea sandstone and Westerly granite, like the previously tested Tennessee marble, showed considerable weakening when subjected to cyclic uniaxial tension. In addition Westerly granite lost strength under cyclic compression even when assisted by confining pressures of 1,000 psi and 2,500 psi.

2. Cyclic uniaxial tension-compression tests in Westerly granite revealed that under such a combination of loading the fatigue strength is considerably weakened. Cyclic tension-compression appeared to be the most devastating type of loading.

3. Based on conclusions 1 and 2, it is clear that hard rock is fatigue prone. Design of structures in rock cannot ignore the effects of repetitive loading. The fatigue strengths of each rock as determined by the reported tests could be used as the effective strengths of intact rocks. Since not every rock in the field can be extensively tested, it is appropriate to suggest an empirical formula based on the results obtained thus far. It is therefore recommended that a value of 50% of the appropriate static strength be used as the effective strength that can withstand static, dynamic and cyclic loading, when rock is subjected only to compression or only to tension. However, when loading takes the form of tension-compression much lower effective strengths should be used. For the stress range

tested in this program 33% of the tensile strength was the fatigue strength at 10^5 cycles. An effective strength of 25% appears reasonable at this time, but will have to be tested for more rocks and stress ranges.

4. "Prefailed" Westerly granite, like the previously tested "prefailed" Georgia and Tennessee marbles, exhibited substantial fatigue endurance, although the fatigue life was reduced when compared with unprefailed rock. The obtained S-N curves could be used to emphasize the importance of considering the strength capacity of failed rock as encountered in underground pillars and walls.

5. Additional experimental evidence was collected in support of an inter-relationship between rock fatigue and the respective complete stress-strain curve. Particularly in granite, the amount of permanent deformation exhibited by the upper peak strain in stress-controlled tests, the shape of the S-N curve, the amount of peak stress relaxation and the type of fatigue failure in strain controlled tests, all allude to a Class II rock type and match the characteristics of the complete stress-strain curve. The practical application of this conclusion cannot be overlooked. Determining the complete stress-strain curve for a rock under specific conditions of loading rate and triaxial stress configuration is much easier and less time consuming than preparing an S-N curve. Monitoring the amount of accumulated permanent deformation at a particular stress level (whether in a laboratory specimen or an underground structure) and comparing it with the allowable magnitude from the complete stress-strain curve, one could evaluate the stability condition and estimate the amount of cyclic loading that the rock can still withstand. The shape of the complete stress-strain curve could indicate the ranges of maximum stress for which the rock is more susceptible to fatigue effects. These are the regions of minimum allowable permanent strain, usually caused by those

portions of the descending stress-strain curve having positive slopes.

6. An additional indication that the maximum allowable permanent strain at a particular upper peak stress actually controls the fatigue endurance of rock was found in tests where the upper peak compressive load was varied in two or three steps during cycling. The total permanent strain for the last maximum stress level used was independent of the loading path, being apparently controlled only by the shape of the complete stress-strain curve.

7. S-N curves for four hard rock types under cyclic uniaxial tension show that they can be represented by a straight line closely averaging S = 100% - 7 log N. This expression could be used to predict fatigue strength for any other hard rock provided the tensile strength (100%) at a loading rate equivalent to the cyclic frequency, is shown.

8. Experiments in uniaxial tension with different cyclic amplitudes for the same upper peak stress showed that the cyclic stress range considerably affects fatigue life.

9. In both tension and compression the permanent strain after the first cycle is always larger than after any other cycle. However, in tension it is so predominent that it averages one half of the total permanent strain at fatigue failure. This result could be effectively used to predict total deformation of a structure before tensile rupture.

10. The investigation of the compression fatigue mechanism shows that the process of cumulative damage is spread through the entire specimen. In uniaxial tension fatigue, hwoever, fabric changes due to cyclic loading appear to be very localized, i.e., a few of the more crucial existing microcracks slowly enlarge until one gains on the others, propagates and splits

the specimen. Other than the very close vicinity of the rupture plane no changes were observed in the internal structure of the rock. The implication here is that unlike compression fatigue, impending tensile fatigue failure may give little warning in terms of deformation away from the critical flaw.

11. In pure cyclic compression or cyclic tension the average tangential Young's modulus decreases between the first and last loading cycles but not by an appreciable amount. In cyclic tension-compression the "softening" of the rock is an impressive 30%. This could be the reason for the appreciable decrease in fatigue strength under tension-compression. It could also help explain the 30% decrease in tensile strength of specimens previously loaded in cyclic tension-compression to 10^5 cycles. Other unfailed specimens pretested in cyclic tension or compression had strengths surprisingly close to those of virgin specimens.

12. The effort of two years as described in the first annual report and in the present final report has, generally, been a very successful one. New knowledge has been gathered in both the engineering aspect and the internal mechanism of fatigue. Some practical applications related to design in rock have been mentioned above. The surprising findings of the tension-compression type loading could possibly be used to advantage in rock drilling. The understanding of the fatigue mechanism and the relationship to the complete stress-strain curve has enhanced the general field of rock mechanics. More work is necessary, however, to complete the originally envisaged three year program, with particular reference to practical applications.

REFERENCES

1. Haimson, B. C., "Mechanical Behavior of Rock under Cyclic Loading", Annual Report, ARPA Contract H0210004 Monitored by the Bureau of Mines, Twin Cities, June 1972.

2. Paterson, M. S., "Triaxial Testing of Materials at Pressures up to 10,000 kg/sq. cm.", J. Inst. Engrs., Australia, Jan.-Feb. 1964.

3. Wawersik, W. R. and Brace, W. F., "Post-Failure Behavior of a Granite and a Diabase", Rock Mech., 3, 1971.

4. Wawersik, W. R., "Detailed Analysis of Rock Failure in Laboratory Compression Tests", Ph. D. Thesis, University of Minnesota, 1968.

5. Burdine, N. T., "Rock Failure under Dynamic Loading Conditions", Soc. of Petr. Engrs. J., March, 1963.

6. Haimson, B. C., Tharp, T. M., "Real Stresses Around Boreholes", SPE 4241, Sixth Conference on Drilling and Rock Mechanics, Austin, Texas, January 1973.